prepared in the CTM. The spleen or MLN T cells (5×10^5) were cultured with 0, 111, 333 or 1000 mg/ml of OVA in the presence of $2{\cdot}5 \times 10^5$ of irradiated (3000 rad) spleen cells from naive C57BL/6 mice in 96-well flat-bottomed culture plates at 37° in 5% CO_2 for 4 days. During the last 18 hr of the 4-day culture, 0·5 μCi of tritiated [^{3}H]thymidine was added to each well. The plates were harvested and counted using a β counter (1450 Microbeta Trilux; Wallac, Gaithersburg, MD).

Cytokine analysis

Levels of IL-4 or IL-2 in the spleen T-cell culture supernatants were analysed by an IL-4-dependent cell line, CT.4S cells (kindly gifted by Prof. William E. Paul, National Institutes of Health, Bethesda, MD), or an IL-2-dependent cell line, CTLL-2 cells (American Type Culture Collection, ATCC, Manassas, VA). T-cell culture supernatants were collected on day 3 and stored frozen at −80° until assay. CT.4S or CTLL-2 cells (5×10^3) were cultured in the presence of the supernatant in 96-well flat-bottomed culture plates at 37° in 5% CO_2 for 3 or 2 days, respectively. To draw a standard curve, CT.4S or CTLL-2 cells were cultured with various quantities of recombinant mouse IL-4 (rIL-4) or rIL-2 (Genzyme, Cambridge, MA), respectively. During the last 18 hr of incubation, 0·5 μCi of [^{3}H]thymidine was added to each well. The plates were harvested and counted using the β counter.

Delayed-type hypersensitivity (DTH) response

Mice were anaesthetized and intradermally injected 20 μg of OVA in 20 μl of saline into the right ears. As negative controls, saline was injected into the left ears. Ear thickness was measured using a dial thickness gauge (Ozaki MFG. Co., LTD. Tokyo, Japan) before and 24 hr after the injection. The swelling rate of the ear was calculated as follows: [(thickness of the ear 24 hr after challenge − thickness of the ear before challenge)/thickness of the ear before challenge] × 100%.

Statistical analysis

Student's *t*-test was used to determine the statistical significance of differences between groups. Data were considered significant at $P < 0{\cdot}05$.

Results

Appearance of detectable OVA antigens in both portal and peripheral blood after oral administration of OVA

The oral administration of OVA induces oral tolerance against OVA, and it has been shown that OVA antigens

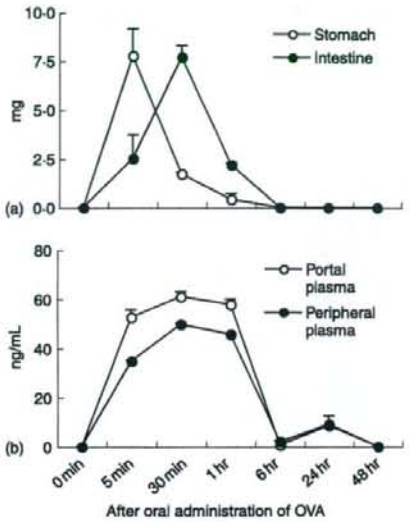

Figure 1. Kinetics of OVA antigens detected in gut contents and plasma after oral administration of OVA. BALB/c mice were orally administered with 25 mg of OVA. At various times after oral administration, the stomach or small intestine contents were collected (a). Portal and peripheral blood was collected from mice at various times after oral administration (b). Levels of OVA antigens in the gut contents or plasma were assessed by ELISA. The data are expressed as the mean + standard error (SE) of three mice.

are detected in peripheral blood after the oral administration of OVA.[30,31] First, we attempted to detect OVA antigens in the digestive tract and in blood after absorption via the guts.

When 25 mg of OVA was orally administered to mice, many OVA antigens in the gastric contents and fewer OVA antigens in the small intestinal contents were detected at 5 min after oral administration (Fig. 1a). While the amount of detectable OVA antigens was reduced at 30 min in the stomach, they reversely increased in the small intestine at the same time. OVA antigens in the guts could not be detected at 6 hr and subsequently (Fig. 1a).

OVA antigens were observed in both portal and peripheral blood at 5 min after the oral administration of OVA (Fig. 1b). They reached a peak at 30 min and became undetected at 6 hr after oral administration (Fig. 1b). Thus, kinetics of OVA antigens in the portal and peripheral blood corresponded to that in the small intestinal contents. The amount of OVA antigens detected in the portal and peripheral blood was dependent on the dose of orally administered OVA (Fig. 2). Levels of OVA antigens in the portal blood were more than in the peripheral blood (Fig. 1b and Fig. 2). OVA antigens were observed in the blood from all strains used in this study, BALB/c, C57BL/6, and BDF_1 mice (data

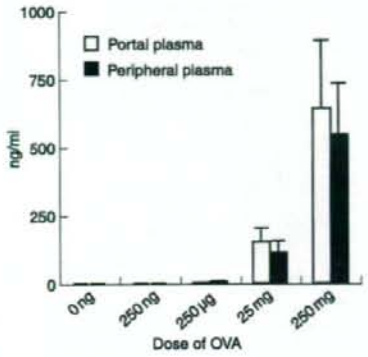

Figure 2. Level of OVA antigens in plasma is dependent on the dose of orally administered OVA. BALB/c mice were orally administered with various doses of OVA. Portal and peripheral blood was collected from mice at 30 min after oral administration. Levels of OVA antigens in plasma were assessed by ELISA. The data are expressed as the mean + SE of three mice.

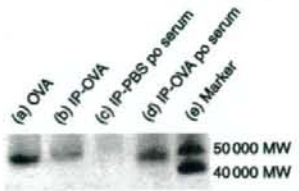

Figure 3. Immunoblot of OVA antigens in the serum after the oral administration of OVA. C57BL/6 mice were orally administered with 250 mg of OVA or PBS. Blood was collected from the heart 30 min after the oral administration (po) of OVA or PBS. OVA antigens in the serum were detected by immunoprecipitation and immunoblotting. Immunoprecipitation was performed using a rabbit anti-OVA polyclonal antibody on serum from mice or OVA mixed with serum from untreated mice. Immunoprecipitated (IP) samples or 2·5 ng of OVA were loaded. Proteins were transferred to a PVDF membrane and detected using the anti-OVA polyclonal antibody. (a) 2·5 ng of OVA, (b) IP sample of OVA mixed with untreated mouse serum, (c) IP sample of the serum after oral administration of PBS, (d) IP sample of the serum after the oral administration of OVA, (e) molecular markers.

not shown). To examine the molecular weights of OVA antigens in the serum, we performed immunoprecipitation and immunoblotting in serum samples using an anti-OVA polyclonal antibody. Surprisingly, 45 000 MW OVA was clearly detected in the serum 30 min after the oral administration of OVA (Fig. 3). In our immunoprecipitation and immunoblotting system using an anti-OVA polyclonal antibody, digested OVA fragments could not be detected in the serum. These results suggest that the macromolecules, 45 000 MW OVA antigens, were absorbed via the small intestines, transferred to the portal vein and circulated in the bloodstream in normal mice, in which oral tolerance was induced.

OVA antigens become undetected in the blood with an increase in mucosal and systemic OVA-specific immunoglobulin

Next, we attempted to analyse OVA antigens in blood from mice induced with OVA-specific immune responses by the oral administration of OVA plus CT adjuvant. Mice were orally administered with 1 or 100 mg of OVA or the same dose of OVA plus CT every week. Peripheral blood samples from mice were collected 30 min after oral administration every week and levels of OVA antigens and OVA-specific IgG in the blood were assessed by ELISA. The production of OVA-specific faecal IgA, OVA-specific T-cell proliferation, and secretion of cytokines were also analysed in mice.

The production of OVA-specific plasma IgG1 and faecal IgA was enhanced after the oral administration of 1 or 100 mg of OVA plus CT; however, the oral administration of OVA without CT did not induce OVA-specific systemic and mucosal antibody production (Fig. 4). OVA-specific serum IgG2a, T helper (Th)1-type antibody, could not be detected by oral administration with and without CT during the experimental period. As shown in Fig. 5, OVA-specific T-cell proliferation was also observed in spleen T cells and MLN T cells from mice orally administered with OVA plus CT (Fig. 5a). IL-4 secretion was observed in culture supernatants from proliferated spleen T cells; however, IL-2 was not

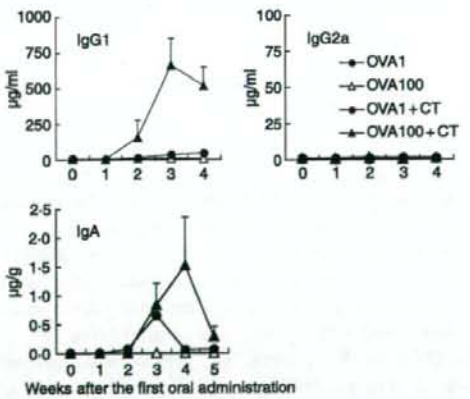

Figure 4. Production of OVA-specific systemic IgG and faecal IgA by oral administration of OVA plus CT. C57BL/6 mice were orally administered with 1 or 100 mg of OVA, or the same dose of OVA plus CT once weekly for 5 weeks. Peripheral blood and faeces were collected from the mice every week. OVA-specific plasma IgG1 and IgG2a and faecal IgA were assessed by ELISA. The data are expressed as the mean anti-OVA immunoglobulin in plasma (μg/ml) or faeces (μg/g) + SE of four mice.

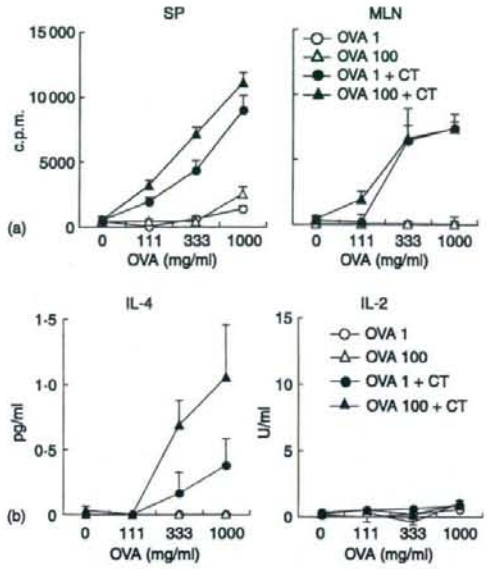

Figure 5. OVA-specific T cell proliferation and secretion of Th2-type cytokine by oral administration of OVA plus CT. C57BL/6 mice were orally administered with 1 mg or 100 mg of OVA, or the same dose of OVA plus CT once weekly for 3 weeks. Spleens and MLNs were removed 2 weeks after the third administration and T cells were isolated. T cells from the spleen or MLN were cultured with 0, 111, 333 or 1000 mg/ml of OVA in the presence of irradiated spleen cells from naive C57BL/6 mice for 4 days. OVA-specific T cell proliferation was assessed as described in Materials and methods (a). Splenic T cell culture supernatants were collected on day 3. IL-4-dependent cell line, CT-4S, or IL-2-dependent cell line, CTLL-2, were cultured in the presence of the supernatant for 3 or 2 days, respectively. Cytokine levels were assessed as described in Materials and methods (b). The results are expressed as the level of orally administered mice minus the level of normal mice. The results are shown as the mean + SE in triplicate. Data are representative of two separate experiments.

detected (Fig. 5b). These results demonstrate that the oral administration of OVA plus CT induces mucosal IgA and Th2-type systemic immune responses.

Although OVA antigens in the blood were sufficiently detected at 1 week after the oral administration of 100 mg of OVA plus CT, they were remarkably reduced at 2 weeks and subsequently remained reduced (Fig. 6), while OVA-specific systemic IgG1 and mucosal IgA were produced (Fig. 4). On the other hand, in mice orally administered with 100 mg of OVA, OVA antigens were detected every week. When 1 mg of OVA or the same dose of OVA plus CT was orally administered, OVA antigens were undetectable in the blood (Fig. 6).

These results show that in immunized mice, mucosal anti-OVA IgA may bind OVA antigens in the gastrointestinal tract and block OVA from entering into the mucosal tissues. Furthermore, OVA antigens may be caught by

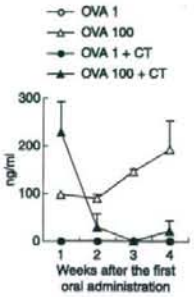

Figure 6. OVA antigens become undetectable after oral administration of OVA plus CT. C57BL/6 mice were orally administered with 1 or 100 mg of OVA or the same dose of OVA plus CT once weekly for 4 weeks. Peripheral blood was collected from the mice 30 min after oral administration every week. OVA antigens in plasma were assessed by ELISA. The data are expressed as the mean + SE of three mice.

anti-OVA IgG and immune complexes might be undetected in ELISA.

Oral administration of intact OVA suppresses OVA-specific immune responses whereas intraportal or intravenous injection cannot induce immunological suppression

The results indicate that OVA antigens appear in the blood from mice in which oral tolerance is induced, although they are markedly reduced in mice in which OVA-specific immune responses are induced. Therefore, we attempted to induce immunological tolerance against OVA by the intravenous injection of OVA. Mice were orally administered or injected into the portal or peripheral vein with 2·5 mg or 25 mg of OVA, and then i.p. immunized with OVA plus alum. OVA-specific systemic immunoglobulin production and DTH response were assessed in the mice.

The oral administration of a high dose of intact OVA significantly suppressed DTH response against OVA ($P < 0.005$), compared with that in the oral treatment of PBS (Fig. 7a). The DTH response, however, was not significantly suppressed by the intraportal or intravenous injection of intact OVA (Fig. 7b, c). When control PBS was injected into ears, DTH response was not induced (Fig. 7).

Oral administration of OVA also significantly suppressed the production of anti-OVA immunoglobulins (Fig. 8a), whereas the production was significantly enhanced rather than suppressed at 1 week after the intraportal or intravenous injection of OVA (Fig. 8b, c). All immunoglobulin subclasses, IgG1, IgG2a, IgG2b, IgM and IgE, were significantly suppressed by the oral administration of OVA (Fig. 8a). On the other hand, in mice injected with OVA intraportally or intravenously, anti-OVA IgG1

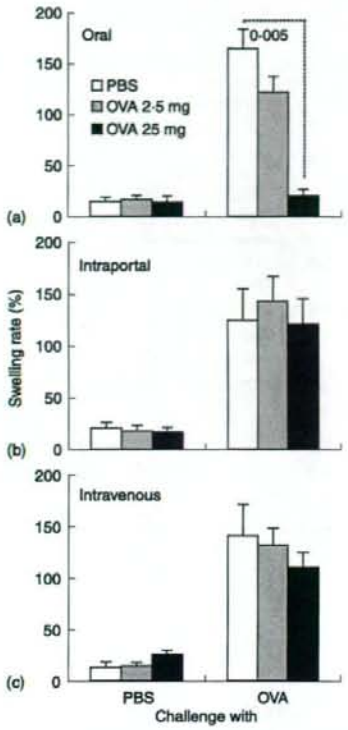

Figure 7. OVA-specific DTH response is suppressed by oral administration of intact OVA, but not by intraportal or intravenous injection of intact OVA. BDF_1 mice were orally administered (a) or injected into the portal (b) or peripheral vein (c) with 2·5 mg or 25 mg of OVA or PBS, and then i.p. immunized with OVA plus alum twice. DTH response was assessed 2 weeks after the second immunization of OVA plus alum. Ear thickness was measured 24 h after challenge of OVA or PBS into the ear. The data are expressed as the mean + SE of five to six mice. The value represents statistical significance ($P <$) compared with control mice treated with PBS in the same way.

at 1 week, IgG2a, IgG2b and IgM were significantly enhanced, although IgG1 at 4 weeks and IgE were suppressed (Fig. 8b, c).

The data clearly show that the injection of intact OVA into the portal or peripheral vein cannot induce immunological tolerance but rather enhances part of immune responses against OVA.

The injection of intact OVA into the lower intestinal tract is less effective in terms of OVA-specific tolerance induction

We therefore investigated whether the modification of intact OVA by gastrointestinal digestion was essential to induce oral tolerance. Mice were orally administered or injected into the guts, stomach, duodenum, ileum, or colon, with 25 mg of intact OVA. OVA-treated and untreated mice were i.p. immunized with OVA plus alum twice, and then OVA-specific plasma immunoglobulin and DTH response were assessed.

OVA-specific immunoglobulin production was remarkably suppressed by the oral administration of intact OVA, whereas immunoglobulin was sufficiently produced in untreated mice (Fig. 9a). The injection of intact OVA into the stomach, duodenum, ileum, or colon significantly enhanced OVA-specific immunoglobulin production ($P < 0·05$), compared with the oral administration of intact OVA (Fig. 9a). DTH response against OVA was also significantly enhanced in mice injected with intact OVA into the ileum or colon ($P < 0·05$ or 0·005, respectively), compared with the oral administration of OVA (Fig. 9b). Levels of OVA-specific immunoglobulins and DTH responses were higher in mice injected with intact OVA into the lower intestinal tract.

The results demonstrate that the appropriate digestion of intact OVA in the gastrointestinal tract is crucial for the induction of oral tolerance against OVA.

Discussion

In this study, we showed that after the oral administration of OVA, OVA antigens were absorbed via the small intestines, transferred into the liver via the portal vein, and circulated in the bloodstream. This suggests that digestive enzymes do not completely digest OVA to amino acids and small peptides that do not have antigenicity, and OVA antigens can cross the intestinal surface.

M cells that exist over PPs uptake soluble macromolecule proteins.[10–12] OVA antigens may be taken up by M cells at the intestinal surface and then they may be processed and presented by immature DCs in PPs, which are shown to be inductive sites for oral tolerance where T cells secreting regulatory cytokines, IL-10[21] and TGF-β,[22] are induced. DCs may capture OVA antigens, present antigen epitopes to naïve T cells, and induce regulatory T cells in PPs. M cells are shown to also exist in small intestinal villi,[37] suggesting that antigens may be taken up by M cells apart from PPs. Moreover, DCs may send dendrites between epithelial cells and acquire OVA antigens over epithelia. Thus, some of the OVA antigens that cross the intestinal surface are captured by DCs in these intestinal mucosal tissues.

A protein antigen is digested by digestive enzymes to amino acids and small peptides.[9] They are absorbed via epithelial cells, and enter the portal vein through capillary vessels in the small intestine. After the oral administration of OVA to mice, OVA antigens are detected in peripheral blood.[30,31] Furthermore, our results clearly showed that OVA antigens, 45 000 MW of proteins, enter the portal vein and then the bloodstream after the oral administration of OVA. OVA antigens taken up by M cells, or using other routes, may enter the portal vein via capillary

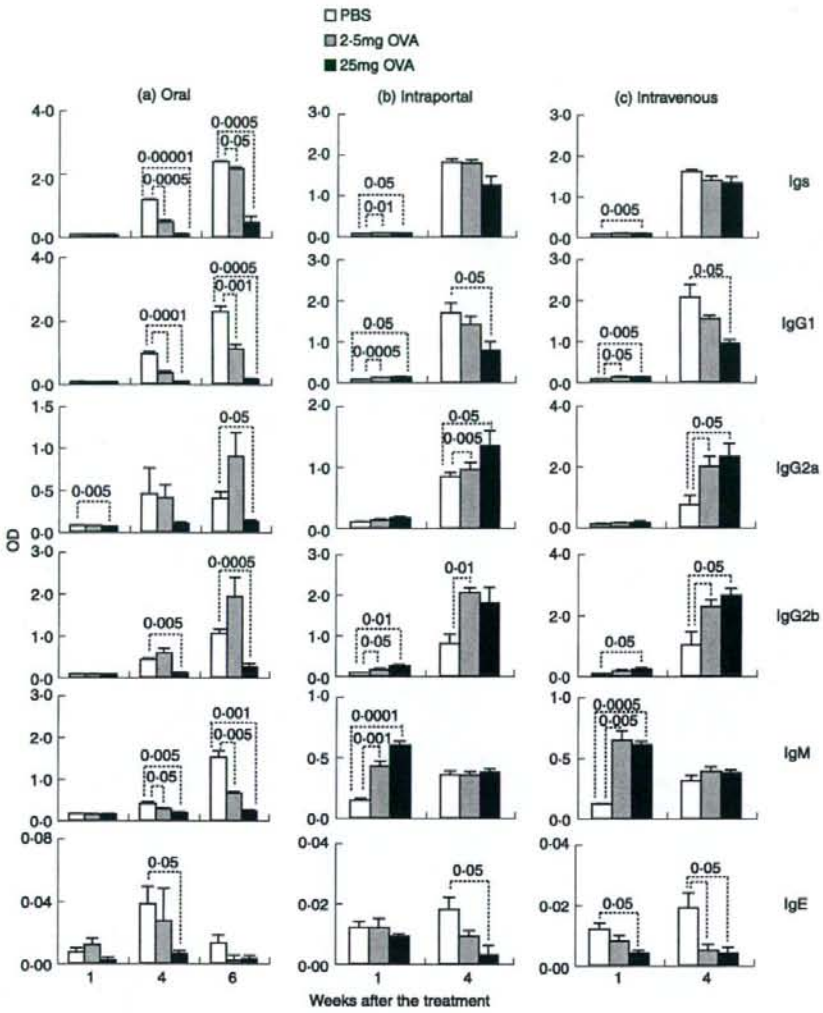

Figure 8. Production of anti-OVA immunoglobulins is suppressed by the oral administration of intact OVA, but not by intraportal or intravenous injection of intact OVA. BDF_1 mice were orally administered (a) or injected into the portal (b) or peripheral vein (c) with 2·5 mg or 25 mg of OVA or PBS. The mice were i.p. immunized with OVA plus alum 1 and 3 weeks after the first oral administration or injection of intact OVA. Orally treated mice were additionally i.p. immunized with OVA 5 weeks after the first oral administration. Peripheral blood was collected at various weeks. Anti-OVA immunoglobulins in plasma were assessed by ELISA. Data are expressed as the mean of OD (415 nm) + SE of five to six mice. Each value represents statistical significance ($P <$), compared with control mice treated with PBS in the same way.

vessels in the small intestine. Some allergens have been shown to cross the mucosal barrier by the disruption of tight junctions.[38,39] Notably, it has been shown that soluble protein antigens are rapidly pinocytosed by enterocytes and co-localized with major histocompatibility complex (MHC) class II in a vesicular compartment.[40] Bland *et al.* proposed that intestinal epithelial cells (IECs) presented antigens on their surface to local T cells[41] and induced suppressor T cells.[42] Recently, it has been reported that tolerosomes, which have an exosome-like structure and carry MHC class II with antigens, were released from IECs into serum.[43] It has also been shown that tolerosome from mouse serum 1 hr after the oral administration of OVA-induced oral tolerance and this induction was MHC class II dependent.[44] Hereafter, it is necessary to examine whether the 45 000 MW OVA antigens detected are free antigens or are included in exosomes in mouse serum.

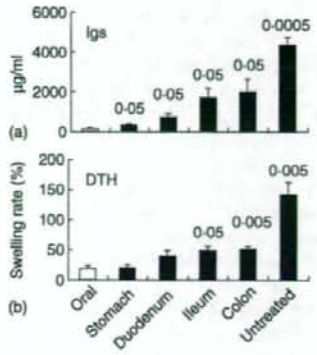

Figure 9. Less effective induction of immunological tolerance by injection of intact OVA into lower intestinal tract. BDF_1 mice were orally administrated or injected into the guts with 25 mg of OVA. OVA-treated and untreated mice were i.p. immunized with OVA plus alum 1 and 3 weeks after OVA treatment. Peripheral blood was collected 1 week after the second immunization of OVA plus alum. Plasma anti-OVA immunoglobulin was assessed by ELISA (a). DTH response against OVA was assessed 6 weeks after the second immunization (b). Data are expressed as the mean + SE of 3–9 mice. Each value represents statistical significance ($P <$), compared with mice orally administered with OVA.

It has been demonstrated that CD25-positive cells are crucial to immunological suppression by the transfer of serum after the oral administration of OVA.[32] The liver has been shown to contribute to tolerance induction because the intraportal injection of allogeneic cells[24,25] eggs of a parasite[26] or insoluble protein[27] induces immunological tolerance against the antigen. It is reported that liver endothelial cells endocytose OVA by a mannose receptor, CD206,[45,46] and antigen presentation by cells induces T-cell tolerance against OVA.[46] In this study, however, the injection of intact OVA into the portal or peripheral vein did not induce immunological tolerance but rather enhanced part of OVA-specific antibody production. As mannose receptors are also expressed on macrophages in red pulp in the spleen[47] intact OVA may be captured by macrophages in the spleen after intravenous injection. In our experimental system, these antigen-presenting cells (APCs) in the liver and spleen may not induce immunological tolerance when they endocytose intact OVA.

The uptake of intact antigens untreated with digestive enzymes may lead to immunological enhancement such as allergy. Ileal injection of BSA treated with pepsin induces immunological tolerance against BSA, whereas ileal injection of intact BSA enhances anti-BSA responses.[48] Correspondingly, in this study, the injection of intact OVA into the ileum or colon significantly enhanced both OVA-specific antibody production and DTH response. Induction of oral tolerance was more difficult when intact OVA was injected into the lower intestinal tract. It is reported that the impairment of gastric digestion of caviar extracts significantly enhanced caviar-specific IgG1, IgG2a, and IgE levels in mice.[49] In addition, cod proteins treated with pepsin show reduced IgE-binding capability and reduced histamine release from human basophils.[50] In the previous study, we demonstrated that oral tolerance against sheep red blood cells (SRBCs) was induced in young mice but rather SRBC-specific antibody response was enhanced in aged mice by the oral administration of SRBC.[51] Digestive and absorptive capacity is decreased in elderly people.[52] Reduced digestive capacity in aged mice might result in the failure of oral tolerance induction. In this report, it was shown that the absolute gastrointestinal ingestion of OVA via the upper gastrointestinal tract is crucial for oral tolerance induction. As macromolecular OVA antigens but not digested antigen fragments are detected in tolerant-mice serum, not only digestion but also some modification of macromolecular OVA in the gastrointestinal tract may be essential for oral tolerance induction.

The detection of OVA antigens has been shown in mouse serum 1 hr after the oral administration of OVA, and serum transfer induced significant suppression of OVA-specific immune responses.[31] Recently, it was shown that tolerosomes including MHC class II are produced by IEC at 1 hr after the oral administration of OVA, and tolerosomes induce oral tolerance.[44] Also in our results, OVA antigens were remarkably detected at 30 min and 1 hr after the oral administration of OVA.

In this study, it was clearly demonstrated that the absolute gastrointestinal ingestion of OVA via the upper gastrointestinal tract is crucial to the establishment of oral tolerance. Although macromolecular OVA antigens are detected after the oral administration of OVA in tolerant-mouse serum, the injection of intact OVA cannot induce tolerance. Therefore, some modification of macromolecular OVA in the gastrointestinal tract and ingestion may be essential for oral tolerance induction.

Acknowledgements

This work was supported in part by a Grant-in-Aid for Young Scientists from the Japan Society for the Promotion of Sciences (JSPS). The authors are grateful to Dr Eiji Shinya, Ms Atsuko Owaki and Dr Megumi Takahashi for advice on the immunoprecipitation and immunoblotting.

References

1 Mowat AM, Strobel S, Drummond HE, Ferguson A. Immunological responses to fed protein antigens in mice. I. Reversal of oral tolerance to ovalbumin by cyclophosphamide. *Immunology* 1982; 45:105–13.

2 Lider O, Santos LM, Lee CS, Higgins PJ, Weiner HL. Suppression of experimental autoimmune encephalomyelitis by

oral administration of myelin basic protein. II. Suppression of disease and in vitro immune responses is mediated by antigen-specific CD8+ T lymphocytes. *J Immunol* 1989; **142**: 748–52.

3 Chehade M, Mayer L. Oral tolerance and its relation to food hypersensitivities. *J Allergy Clin Immunol* 2005; **115**: 3–12; quiz 3.

4 Breiteneder H, Ebner C. Molecular and biochemical classification of plant-derived food allergens. *J Allergy Clin Immunol* 2000; **106**(1 Part 1):27–36.

5 Sicherer SH, Sampson HA. 9. Food allergy. *J Allergy Clin Immunol* 2006; **117**(2 Suppl.):S470–5.

6 Khakoo A, Lack G. Preventing food allergy. *Curr Allergy Asthma Rep* 2004; **4**:36–42.

7 Weiner HL, Friedman A, Miller A *et al.* Oral tolerance: immunologic mechanisms and treatment of animal and human organ-specific autoimmune diseases by oral administration of autoantigens. *Annu Rev Immunol* 1994; **12**:809–37.

8 Ma S, Jevnikar AM. Autoantigens produced in plants for oral tolerance therapy of autoimmune diseases. *Adv Exp Med Biol* 1999; **464**:179–94.

9 Erickson RH, Kim YS. Digestion and absorption of dietary protein. *Annu Rev Med* 1990; **41**:133–9.

10 Bockman DE, Cooper MD. Pinocytosis by epithelium associated with lymphoid follicles in the bursa of Fabricius, appendix, and Peyer's patches. An electron microscopic study. *Am J Anat* 1973; **136**:455–77.

11 von Rosen L, Podjaski B, Bettmann I, Otto HF. Observations on the ultrastructure and function of the so-called 'microfold' or 'membraneous' cells (M cells) by means of peroxidase as a tracer. *Virchows Arch a Pathol Anat Histol* 1981; **390**:289–312.

12 Neutra MR, Phillips TL, Mayer EL, Fishkind DJ. Transport of membrane-bound macromolecules by M cells in follicle-associated epithelium of rabbit Peyer's patch. *Cell Tissue Res* 1987; **247**:537–46.

13 Wolf JL, Kauffman RS, Finberg R, Dambrauskas R, Fields BN, Trier JS. Determinants of reovirus interaction with the intestinal M cells and absorptive cells of murine intestine. *Gastroenterology* 1983; **85**:291–300.

14 Sicinski P, Rowinski J, Warchol JB, Jarzabek Z, Gut W, Szczygiel B, Bielecki K, Koch G. Poliovirus type 1 enters the human host through intestinal M cells. *Gastroenterology* 1990; **98**:56–8.

15 Amerongen HM, Weltzin R, Farnet CM, Michetti P, Haseltine WA, Neutra MR. Transepithelial transport of HIV-1 by intestinal M cells: a mechanism for transmission of AIDS. *J Acquir Immune Defic Syndr* 1991; **4**:760–5.

16 Owen RL, Pierce NF, Apple RT, Cray WC Jr. M cell transport of *Vibrio cholerae* from the intestinal lumen into Peyer's patches: a mechanism for antigen sampling and for microbial transepithelial migration. *J Infect Dis* 1986; **153**:1108–18.

17 Grutzkau A, Hanski C, Hahn H, Riecken EO. Involvement of M cells in the bacterial invasion of Peyer's patches: a common mechanism shared by *Yersinia enterocolitica* and other enteroinvasive bacteria. *Gut* 1990; **31**:1011–5.

18 Jones BD, Ghori N, Falkow S. *Salmonella typhimurium* initiates murine infection by penetrating and destroying the specialized epithelial M cells of the Peyer's patches. *J Exp Med* 1994; **180**:15–23.

19 Kelsall BL, Strober W. Distinct populations of dendritic cells are present in the subepithelial dome and T cell regions of the murine Peyer's patch. *J Exp Med* 1996; **183**:237–47.

20 Rescigno M, Urbano M, Valzasina B *et al.* Dendritic cells express tight junction proteins and penetrate gut epithelial monolayers to sample bacteria. *Nat Immunol* 2001; **2**:361–7.

21 Fujihashi K, Dohi T, Rennert PD, Yamamoto M, Koga T, Kiyono H, McGhee JR. Peyer's patches are required for oral tolerance to proteins. *Proc Natl Acad Sci USA* 2001; **98**: 3310–5.

22 Tsuji NM, Mizumachi K, Kurisaki J. Antigen-specific, $CD4^+$ $CD25^+$ regulatory T cell clones induced in Peyer's patches. *Int Immunol* 2003; **15**:525–34.

23 Spahn TW, Fontana A, Faria AM *et al.* Induction of oral tolerance to cellular immune responses in the absence of Peyer's patches. *Eur J Immunol* 2001; **31**:1278–87.

24 Nakano Y, Monden M, Valdivia LA, Gotoh M, Tono T, Mori T. Permanent acceptance of liver allografts by intraportal injection of donor spleen cells in rats. *Surgery* 1992; **111**:668–76.

25 Yu S, Nakafusa Y, Flye MW. Portal vein administration of donor cells promotes peripheral allospecific hyporesponsiveness and graft tolerance. *Surgery* 1994; **116**:229–34; discussion 34–5.

26 Cuison A, Tasaka K, Chuang CK, Minai M, Yoshikawa H, Nakajima Y. Schistosome eggs in the portal vein can induce tolerance. *Int J Parasitol* 1995; **25**:993–8.

27 Ogasawara H, Watari E, Shirai Y, Yokomuro K. [Inhibitory effects of portal venous injection of type II collagen in collagen-induced arthritis]. *Nippon Ika Daigaku Zasshi* 1997; **64**:220–4.

28 May CD, Remigio L, Feldman J, Bock SA, Carr RI. A study of serum antibodies to isolated milk proteins and ovalbumin in infants and children. *Clin Allergy* 1977; **7**:583–95.

29 Vance GH, Thornton CA, Bryant TN, Warner JA, Warner JO. Ovalbumin-specific immunoglobulin G and subclass responses through the first 5 years of life in relation to duration of egg sensitization and the development of asthma. *Clin Exp Allergy* 2004; **34**:1542–9.

30 Bruce MG, Ferguson A. The influence of intestinal processing on the immunogenicity and molecular size of absorbed, circulating ovalbumin in mice. *Immunology* 1986; **59**:295–300.

31 Peng HJ, Turner MW, Strobel S. The generation of a 'tolerogen' after the ingestion of ovalbumin is time-dependent and unrelated to serum levels of immunoreactive antigen. *Clin Exp Immunol* 1990; **81**:510–5.

32 Karlsson MR, Kahu H, Hanson LA, Telemo E, Dahlgren UI. Tolerance and bystander suppression, with involvement of CD25-positive cells, is induced in rats receiving serum from ovalbumin-fed donors. *Immunology* 2000; **100**:326–33.

33 Kato H, Fujihashi K, Kato R, Yuki Y, McGhee JR. Oral tolerance revisited: prior oral tolerization abrogates cholera toxin-induced mucosal IgA responses. *J Immunol* 2001; **166**:3114–21.

34 Wakabayashi A, Eishi Y, Nakamura K. Development of the immune system in severe combined immunodeficiency mice reconstituted with transferred fetal liver cells. *J Med Dent Sci* 1997; **44**:21–9.

35 Wakabayashi A, Eishi Y, Nakamura K. Regulation of experimental autoimmune orchitis by the presence or absence of testicular antigens during immunological development in SCID mice reconstituted with fetal liver cells. *Immunology* 1997; **92**:84–90.

36 Kweon MN, Fujihashi K, VanCott JL, Higuchi K, Yamamoto M, McGhee JR, Kiyono H. Lack of orally induced systemic unresponsiveness in IFN-gamma knockout mice. *J Immunol* 1998; **160**:1687–93.

37 Jang MH, Kweon MN, Iwatani K *et al.* Intestinal villous M cells: an antigen entry site in the mucosal epithelium. *Proc Natl Acad Sci USA* 2004; **101**:6110–5.

38 Wan H, Winton HL, Soeller C *et al.* Der p 1 facilitates transepithelial allergen delivery by disruption of tight junctions. *J Clin Invest* 1999; **104**:123–33.

39 Mine Y, Zhang JW. Surfactants enhance the tight-junction permeability of food allergens in human intestinal epithelial Caco-2 cells. *Int Arch Allergy Immunol* 2003; **130**:135–42.

40 Gonnella PA, Wilmore DW. Co-localization of class II antigen and exogenous antigen in the rat enterocyte. *J Cell Sci* 1993; **106**:937–40.

41 Bland PW, Warren LG. Antigen presentation by epithelial cells of the rat small intestine. I. Kinetics, antigen specificity and blocking by anti-Ia antisera. *Immunology* 1986; **58**:1–7.

42 Bland PW, Warren LG. Antigen presentation by epithelial cells of the rat small intestine. II. Selective induction of suppressor T cells. *Immunology* 1986; **58**:9–14.

43 Karlsson M, Lundin S, Dahlgren U, Kahu H, Pettersson I, Telemo E. 'Tolerosomes' are produced by intestinal epithelial cells. *Eur J Immunol* 2001; **31**:2892–900.

44 Ostman S, Taube M, Telemo E. Tolerosome-induced oral tolerance is MHC dependent. *Immunology* 2005; **116**:464–76.

45 Kindberg GM, Magnusson S, Berg T, Smedsrod B. Receptor-mediated endocytosis of ovalbumin by two carbohydrate-specific receptors in rat liver cells. The intracellular transport of ovalbumin to lysosomes is faster in liver endothelial cells than in parenchymal cells. *Biochem J* 1990; **270**:197–203.

46 Limmer A, Ohl J, Kurts C *et al.* Efficient presentation of exogenous antigen by liver endothelial cells to $CD8^+$ T cells results in antigen-specific T-cell tolerance. *Nat Med* 2000; **6**:1348–54.

47 Linehan SA, Martinez-Pomares L, Stahl PD, Gordon S. Mannose receptor and its putative ligands in normal murine lymphoid and nonlymphoid organs: In situ expression of mannose receptor by selected macrophages, endothelial cells, perivascular microglia, and mesangial cells, but not dendritic cells. *J Exp Med* 1999; **189**:1961–72.

48 Michael JG. The role of digestive enzymes in orally induced immune tolerance. *Immunol Invest* 1989; **18**(9–10):1049–54.

49 Untersmayr E, Scholl I, Swoboda I *et al.* Antacid medication inhibits digestion of dietary proteins and causes food allergy: a fish allergy model in BALB/c mice. *J Allergy Clin Immunol* 2003; **112**:616–23.

50 Untersmayr E, Poulsen LK, Platzer MH, Pedersen MH, Boltz-Nitulescu G, Skov PS, Jensen-Jarolim E. The effects of gastric digestion on codfish allergenicity. *J Allergy Clin Immunol* 2005; **115**:377–82.

51 Wakabayashi A, Utsuyama M, Hosoda T, Sato K, Hirokawa K. Differential age effect of oral administration of an antigen on antibody response: an induction of tolerance in young mice but enhancement of immune response in old mice. *Mech Ageing Dev* 1999; **109**:191–201.

52 Masamune O. Digestive and absorptive capacity in the elderly. *Rinsho Byori* 1989; **37**:629–33.

Biophysical Journal Volume 92 April 2007 2570–2582

Molecular Analysis of TCR and Peptide/MHC Interaction Using P18-I10-Derived Peptides with a Single D-Amino Acid Substitution

Yohko Nakagawa,* Hiroto Kikuchi,† and Hidemi Takahashi*
*Department of Microbiology and Immunology and †Department of Physics, Nippon Medical School, Tokyo 113-8602, Japan

ABSTRACT For the structural analysis of T-cell receptor (TCR) and peptide/MHC interaction, a series of peptides with a single amino acid substitution by a corresponding D-amino acid, having the same weight, size, and charge, within P18-I10 (aa318–327: RGPGRAFVTI), an immunodominant epitope of HIV-1 IIIB envelope glycoprotein, restricted by the H-2D^d class I MHC molecule, has been synthesized. Using those peptides, we have observed that the replacement at positions 324F, 325V, 326T, and 327I with each corresponding D-amino acid induced marked reduction of the potency to sensitize targets for P18-I10-specific murine CD8$^+$ cytotoxic T lymphocytes (CTLs), LINE-IIIB, recognition. To analyze further the role of amino acid at position 325, the most critical site for determining epitope specificity, we have developed a CTL line [LINE-IIIB(325D)] and its offspring clones specific for the epitope I-10(325v) having a D-valine (v) at position 325. Taking advantage of two distinct sets of CD8$^+$ CTLs restricted by the same D^d, three-dimensional structural analysis on TCR and peptide/MHC complexes by molecular modeling was performed, which indicates that the critical amino acids within the TCRs for interacting with 325V or 325v appear to belong to the complementarity-determining region 1 but not to the complementarity-determining region 3 of Vβ chain.

INTRODUCTION

Immune responses to viral infection include both humoral and cell-mediated effector mechanisms. The major effector cells in cellular immunity are CD8 molcule-expressing cytotoxic T lymphocytes (CTLs) that can recognize and kill virus-infected cells. In general, endogenously synthesized antigens such as virus-derived proteins are fragmented inside of the cells and are presented on the cell in conjunction with class I major histocompatibility complex (MHC) molecules. Such processed epitope peptides associated with the class I MHC molecules can be recognized by CTLs via their specific T cell receptors (TCRs).

The TCRs expressed on the cell surface of T lymphocytes contain similar structural patterns with immunoglobulin-like domains, comprising one variable and one constant, as well as a transmembrane domain and a short cytoplasmic tail. The specificity for T-cell recognition seems to be determined by the variable domains, TCR Vα and TCR Vβ, within two heterodimeric subsets, TCRα and TCRβ. Several recent findings have indicated that the TCRα and β heterodimers are oriented to the long axis of the epitope-peptide/MHC complex (1), in which the Vα domain appears to cover the amino-terminal half of the epitope peptide, whereas Vβ is located over the carboxyl-terminal portion of the epitope (2).

Among those variable Vα and Vβ domains, three hypervariable complementarity-determining regions (CDRs), termed CDR1, CDR2, and CDR3, seem to directly interact with the peptide/MHC complex. Because the degree of variability is the greatest in the CDR3 loop generally, and it is positioned more closely over the epitope peptide than other CDR1 and CDR2 loops, the antigen specificity has been considered to be associated with the CDR3 but not with CDR1 or CDR2, which were predicted to interact principally with the MHC molecules (3,4). Indeed, according to a recent report on the murine K^b class I MHC molecule-restricted epitope octapeptide (pKB1: KVITFIDL) recognized by KB5-C20 TCR (5), TCR plasticity is primarily restricted to the CDR3 loops of the Vβ domain. Nevertheless, recent crystallographic analyses on various TCR and peptide/MHC interactions have suggested the possibility of direct contact for both CDR1 and CDR3 in the TCRα and TCRβ chains with the antigenic peptide/MHC complex (5,6). Therefore, to understand more precise molecular interactions determining T-cell specificity through TCR-mediated peptide/MHC complex recognition, we took advantage of the following known materials to accomplish the analysis.

We have established CD8$^+$, H-2D^d class I MHC molecule-restricted murine CTL line, LINE-IIIB, specific for the envelope glycoprotein 160 (gp160) composed of ~900 amino acids derived from one of the most commonly used IIIB strains of human immunodeficiency virus type-1 (HIV-1), a causative agent for acquired immunodeficiency syndrome (AIDS) (7). Then, we have identified an immunodominant epitope within the gp160 as a 15-residue peptide, P18IIIB (aa315–329: RIQRGPGRAFVTIGK), for the LINE-IIIB recognition (7) as well as the minimal active 10-residue peptide, P18-I10 (aa318–327: RGPGRAFVTI) within P18IIIB (8). Moreover, although the position of P18IIIB is located in the hypervariable portion (termed V3 domain) of the viral envelope, the site has turned out to be recognized by various isolate-specific CTLs in an isolate-specific manner (9,10), and

Submitted August 16, 2006, and accepted for publication December 13, 2006.

Address reprint requests to Hidemi Takahashi, Department of Microbiology and Immunology, Nippon Medical School, 1-1-5 Sendagi, Bunkyo-ku, Tokyo 113-8602, Japan. Tel.: 81-3-3822-2131 ext. 5381; Fax: 81-3-3316-1904; E-mail: htkuhkai@nms.ac.jp.

0006-3495/07/04/2570/13 $2.00

doi: 10.1529/biophysj.106.095208

a number of distinct class I MHC molecules did present the P18IIIB to each specific CTL (11). Furthermore, the P18IIIB in the V3-domain was found to be overlapped with the major determinant sites for neutralizing antibodies against HIV-1 in an isolate-specific manner (12–14) and also to be recognized by CD4-positive helper T lymphocytes specific for HIV-1 in a class II MHC molecule-restricted manner (8,15). In addition, human CTLs did see the P18IIIB when presented by HLA A2 and A3 (16). These findings indicate that the P18IIIB appears to be a highly attractive epitope for the development of peptide-based vaccine against AIDS, and thus, it is important to study the precise interaction between the epitope P18IIIB and their specific TCRs to study the manner of T-cell-mediated immune responses.

Using a series of peptides with an alanine (A) substitution at each position, we observed that amino acids at positions 322R and position 324F were critical for D^d binding and that position 325V within P18-I10 was essential for interacting with TCRs (17). Also, C-terminus 327I appears to be critical for D^d binding to form the D^d-binding motif (8,18). In addition, we found the HIV-MN isolate-specific CTLs also saw the corresponding minimal active site, MNT10 (aa318–327: IGPGRAFYTT) in association with the same D^d molecules, and replacement of just a single residue, 325V with 325Y, within the P18-I10 or vice versa within the MNT10 was sufficient to reciprocally interchange the specificities for these two non-cross-reactive sets of CTLs (9,10). Thus, a single side chain at position 325 can play a critical role in determining the epitope specificity within both P18-I10 and MNT10 presented by the same class I MHC molecule D^d for $CD8^+$ CTL TCR recognition mediated by the CDRs.

It has been reported that the charge of the amino acid might also affect interaction between TCRs and peptide/MHC complexes (19). Indeed, when negatively charged glutamic acid (E) at position 436 within HIV-1-envelope-derived helper T-cell epitope T1 (aa428–443; KQIINMWQEVGKAMYA) (20) was substituted with either uncharged alanine (A) or size-conservative, uncharged glutamine (Q), stimulatory capacity of the substitute peptides for T1-specific T hybridomas was significantly enhanced, although charge-conservative aspartic acid (D) substitution did not show any enhancement (21). Moreover, substitution at position 6Q in the immunodominant CTL epitope for vesicular stomatitis virus (RGYVYQGL, VSV8) presented by K^d class I MHC molecules to a negatively charged residue such as 6E or 6D induced a change at position 93S of TCR CDR3α to a positively charged residue 93R or 93K (22). Therefore, particularly to reduce the influence of charges of each amino acid as well as the size and molecular weight on TCR-mediated recognition, a series of P18-I10-derived peptides with a single amino acid substitution by D-amino acid at each corresponding site have been synthesized. Using those D-amino acid–substituted peptides, we found apparent reduction of specific cytotoxic activity in the 325V-specific LINE-IIIB cells by the replacement of 325V with D-type valine at position 325, represented as I10(325v). Then, we attempted to establish CTL lines specific for the epitope I-10(325v) by immunization with dendritic cells pulsed with the peptide, I10(325v) (23). We have successfully generated both a 325(v)-specific CTL line and clones that did not cross-react with the original P18-I10.

Taking advantage of two distinct sets of $CD8^+$ CTL clones specific for either P18-I10 bearing L-type valine or I10(325v) having D-type valine at position 325 presented by the same MHC molecules D^d, we attempted to study the three-dimensional (3D) structural analysis on TCRs and peptide/MHC complexes. Here, using molecular modeling analysis, we would like to show that the critical amino acids for interacting with P18-I10 in determining epitope specificity appear to be the peptide DMSHET within CDR1 of Vβ7, whereas those for interacting with I10(325v) appear to be TNSHNY within CDR1 of Vβ8.3.

MATERIALS AND METHODS

Mice

Female BALB/c (H-2^d) mice were purchased from Charles-River Japan Inc. (Tokyo, Japan). The mice were 6 to 10 weeks of age and were maintained in a specific-pathogen-free environment. All experiments were performed according to the guidelines of the NIH Guide for the Care and Use of Laboratory Animals.

Synthetic peptides

Peptides were synthesized and purified as described previously (24). Table 1 summarizes the peptides used in this study; L-amino acids are represented as capital letters, and D-amino acids as lower-case letters.

Transfectants

BALB/c.3T3 (H-2^d) fibroblast transfectants expressing the HIV-1 gp160 of IIIB isolate (15-12) and control transfectants with selectable marker genes (Neo) (7, 17) were used for the CTL assay. Murine L-cells (H-2^k) transfected with H-$2D^d$ (T4.8.3) (25), H-$2L^d$ (T.1.1.1) (25), and H-$2K^d$ (B4III2) (26) were used to determine the MHC class I restriction of the generated CTL line and clones.

Monoclonal antibodies

We used fluorescein isothiocyanate-conjugated antimouse CD3 (145-2C11), $\alpha\beta$TCR (H57-597), CD4 (RM4-5), and CD8 (53-6.7) monoclonal antibodies (PharMingen, San Diego, CA) to determine the cell surface molecules of the established CTL lines and clones.

CTL lines and clones

The P18-I10-specific CTL line, LINE-IIIB, was generated as described previously (7). Based on a previously reported procedure (23), a CTL line specific for I10(325v) was generated from spleen cells of BALB/c mice immunized with I10(325v)-pulsed splenic dendritic cells. Briefly, immune spleen cells were restimulated in vitro with mitomycin C-treated I10(325v)-pulsed syngeneic BALB/c.3T3 fibroblasts in 24-well culture plates containing 1.5 ml of complete T-cell medium composed of RPMI 1640 medium

TABLE 1 Sequences of substituted peptides used in this study

Peptide	Sequence*															
Residue No.	315										325					329
P18IIIB	R	I	Q	R	G	P	G	R	A	F	V	T	I	G	K	
P18-I10				R	G	P	G	R	A	F	V	T	I			
I10(325I)											I					
I10(325L)											L					
I10(325A)											A					
I10(325Y)											Y					
I10(325F)											F					
I10(325H)											H					
I10(325T)											T					
I10(325S)											S					
I10(325E)											E					
I10(325K)											K					
I10(325R)											R					
I10(325P)											P					
I10(318r)				r												
I10(320p)						p										
I10(322r)								r								
I10(323a)									a							
I10(324f)										f						
I10(325v)											v					
I10(326t)												t				
I10(327i)													i			
I10(325v)				R	G	P	G	R	A	F	v	T	I			
I10(325i)											i					
I10(325l)											l					
I10(325a)											a					
I10(325y)											y					
I10(325f)											f					
I10(325h)											h					
I10(325t)											t					

*Sequences of substituted peptides are derived from and aligned with the sequence of P18-I10, an immunodominant epitope of HIV-1 gp160 envelope glycoprotein of the IIIB strain for the H-2D^d-restricted murine CTL. In these peptides, L-amino acids are expressed as capital letters and corresponding D-amino acids are expressed as small letters.

supplemented with 2 mM L-glutamine, 50 μM 2-ME, 100 U/ml penicillin, 100 μg/ml streptomycin, 10% heat-inactivated FCS, and 10% Rat T-STIM (Collaborative Biomedical Products, Bedford, MA). To establish CTL lines, the generated CTLs were maintained by biweekly stimulation with the mitomycin C-treated I10(325v)-pulsed Neo and were termed LINE-IIIB(325D) cells. CTL clones were established from bulk CTL lines using a limiting dilution technique in 96-well U-bottomed microplates, as described previously (15).

CTL assay

The cytolytic activity of the CTL lines and clones was measured, as previously described (27), using a standard 5-h ^{51}Cr-release assay with various ^{51}Cr-labeled targets, as indicated in the figure legends.

Flow cytometric analysis

Flow cytometric analysis was performed to determine the surface molecule expression of the established CTL lines and clones using a FACScan analyzer (Becton Dickinson Immunochemical Systems, Mountain View, CA). We harvested 5×10^5 cells, washed them twice with serum-free RPMI 1640, and then pelleted them. Fluorescein isothiocyanate-conjugated monoclonal antibodies were added to pellets, and they were then incubated for 30 min at 4°C. Then, the cells were washed three times and resuspended with phosphate-buffered saline (PBS) containing 0.1% bovine serum albumin and 0.1% sodium azide. Dead cells were gated out by forward and side scatter based on propidium iodide uptake. Ten thousand events were acquired for each sample and analyzed using Cell Quest software (Becton Dickinson, Franklin Lakes, NJ).

mRNA extraction, reverse transcription, and PCR amplification

Poly(A) tail-bearing mRNA was isolated from CTL clones using the Fast Track mRNA Isolation Kit (Invitrogen, Carlsbad, CA) according to the manufacturer's instructions. Reverse transcription and PCR amplification of purified mRNA were performed with a GeneAmp RNA PCR Kit (PE Biosystems, Foster City, CA). For the synthesis of T-cell receptor Vβ-specific cDNA, Vβ7-specific primer (ACATCCCTAAAGGATACAGGG) and Vβ8-specific primer (ATATCCCTGATGGGTACAAGG) were used in conjunction with Cβ primer (CCGATGGGAGCACACGAACCCTTAAG). For the synthesis of T-cell receptor Vα-specific cDNA, Vα2-specific primer (AGCAATTCTGAACTGCAGTTA), Vα3-specific primer (CAGCCCGATGCTCGCGTCACT), and Vα16-specific primer (ATGGACTGTGTGTATGAAAC) were used in conjunction with Cα primer (ACTGGACCACAGCCTCAGCGTC).

DNA sequence analysis

PCR products were separated by electrophoresis on a 1% of agarose gel and sliced bands were purified by EASYTRAP glass powder (Takara Bio., Siga, Japan). We then analyzed the purified DNA by a direct-sequence technique, using the ABI PRISM Big Dye Terminator Cycle Sequencing FS Ready Reaction Kit (PE Biosystems), and we analyzed the sequences on the ABI PRISM 377XL DNA Sequencing System (PE Biosystems).

Molecular modeling

Because the actual 3D TCR structures for both Vβ7 and Vβ8.3 were unknown, we carried out comparative and homology modeling to elucidate the spatial relation between TCRβ (Vβ7 or Vβ8.3) and P18-I10 or I10(325v). Comparative modeling predicts the 3D structure of a given protein sequence (target) primarily on the basis of its alignment to one or more proteins of a known 3D structure (templates). It is usually difficult to accurately determine the 3D structure from a protein sequence by theoretical procedures. However, because the 3D TCRβ structure consists of a sandwich comprising a four-stranded antiparallel β-sheet and a three-stranded antiparallel β-sheet that are linked by a disulfide bond, and because the core portion was tightly bound by a hydrogen bond, the 3D structure of the TCRβ, especially the core portion, could be reliably predicted.

Following the above procedure, the so-called threading or 3D template-matching method (28) could be implemented to select templates. For this procedure, we used LIBRA (29) (http://www.ddbj.nig.ac.jp/search/libra_i-e.html) software in which compatible structures of a target sequence are sought from the structural library chosen from the Protein Data Bank (PDB), and the target sequence and 3D profile are aligned by simple dynamic programming. According to the alignment, sequence remounts on the structure and its fitness are evaluated by the pseudoenergy potential. The scores are then sorted from the best-matched templates and shown along with their alignments. Based on the obtained alignments between the template and the target Vβ sequence, a 3D model is calculated by the MODELLER software (30–33), by which five 3D models were obtained from five templates used.

To examine the interaction between the calculated TCR and P18-I10, TCR/peptide/class I MHC complex (PDB code 1kj2) was used for two reasons. First, the 3D structure of the MHC part of 1kj2 is almost identical to that of MHC used in our experiment, which is also resolved (code 1bii) and shows a H-2D^d class I MHC molecule presenting the HIV-derived peptide

P18-I10 (RGPGRAFVTI) (34). The amino acid sequence identity between 1kj2 and 1bii is ~90%. Second, 1kj2 is a TCR/peptide/MHC complex (5), whereas 1bii is only a peptide/MHC complex. In our 3D models, Vβ7 or Vβ8.3 was fitted to the TCRβ position in 1kj2 and was drawn by Mol Feat software (FiatLux, Tokyo, Japan).

Quantum chemical calculation

To study the effect of electric charge on the TCR recognition response, we calculated both the electronic state of P18-I10 and any changes therein based on a single amino acid substitution (325V with 325T) within the P18-I10 using the PM5 molecular orbital method (MOPAC2002) (35). In this calculation, hydrogen atoms were first added to the PDB 3D structures, and then the net charges of all atoms in them were obtained, with the PDB 3D structure being maintained.

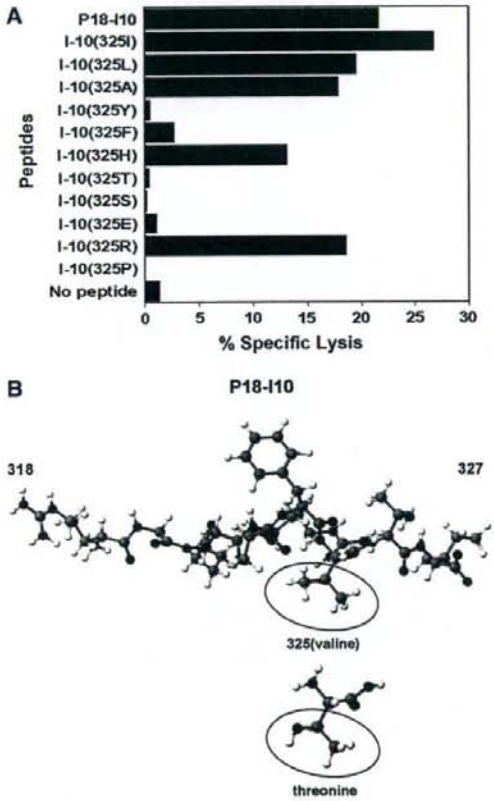

FIGURE 1 Effect of a single amino acid substitution at position 325 within P18-I10 on LINE-IIIB recognition. (*A*) Ten thousand of P18-I10-specific CTL line (LINE-IIIB cells) were added to 5000 ^{51}Cr-labeled BALB/c.3T3 fibroblast target cells in the presence of 3 μM of the substituted peptides at position 325 within P18IIIB, as shown in Table 1. Standard errors of the means of triplicate cultures were <5% of the mean in each case. Results are representative of three independent experiments. (*B*) Ball-and-stick model of peptide P18-I10. The amino acid side chain containing the valine (V) at position 325 within P18-I10 and threonine (T) are shown in the circle. Carbon, oxygen, nitrogen, and hydrogen are shown in gray, red, blue, and white, respectively.

RESULTS

Effect of a single amino acid substitution at position 325 within P18-I10 on LINE-IIIB recognition

First, to see the effect of a single amino acid substitution at position 325 where epitope specificity for LINE-IIIB recognition is determined, a series of P18-I10-derived peptides shown in Table 1 have been synthesized. Similar to our previous findings (10), we confirmed that LINE-IIIB cross-reacted with an aliphatic residue, such as I, L, or A at position 325, in addition to reacting with the original residue V. Moreover, LINE-IIIB cross-reacted with positively charged residues such as R and H but not with the negatively charged E or the uncharged T, S, or P at position 325 (Fig. 1 *A*). Here, we should focus on the case of T, because the 3D structure of the side chain of T is very similar to that of V. When only one carbon atom of the side chain of V is exchanged for one oxygen atom (Fig. 1 *B*; *red*), the amino acid becomes T, except for the hydrogen atoms. According to the quantum chemical calculation using Hamiltonian PM5, the net charge of the carbon atom in V was about $-0.3e$, whereas that of the oxygen atom in T is about $-0.4e$; e represents the elementary charge. This may be the reason why the recognition of V at position 325 by LINE-IIIB was dramatically changed by substitution with T. These results indicate that the charges of the amino acids within the epitope may affect the interaction between TCRs and peptide/MHC complexes.

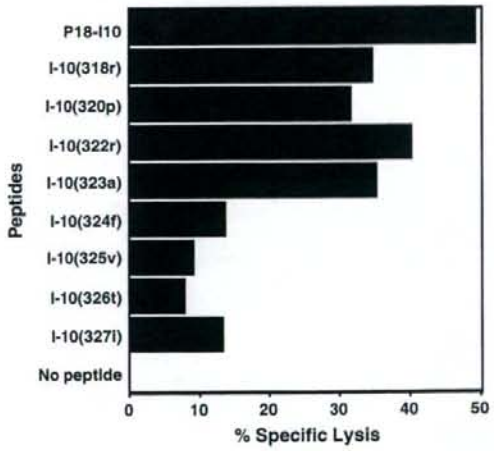

FIGURE 2 Effect of a single amino acid substitution with D-amino acid within an epitope peptide, P18-I10, on LINE-IIIB recognition. Ten thousand LINE-IIIB cells were added to 5000 ^{51}Cr-labeled BALB/c.3T3 fibroblast target cells in the presence of 3 μM of the substituted peptides with a single amino acid substitution by D-amino acid at each corresponding site (represented by lower-case letters in Table 1). Standard errors of the means of triplicate cultures were <5% of the mean in each case. Each experiment was performed at least three times.

Effect of a single amino acid substitution with D-amino acid within an epitope peptide, P18-I10, on LINE-IIIB recognition

Second, to examine the effect of amino acid substitution with the same weight and charged D-amino acid on LINE-IIIB recognition, a series of P18-I10-derived peptides with a single amino acid substitution by D-amino acid at each corresponding site represented by small letters in Table 1 has also been synthesized. When the corresponding D-amino acid was substituted at position 324, 325, 326, or 327, the cytotoxic activity of LINE-IIIB was markedly reduced when compared with other substituted peptides (Fig. 2). This finding suggests that CTL-TCRs can strictly recognize each amino acid within the C-terminal half of the epitope peptide, including at position 325, which is critical for determining epitope specificity, and this is in contrast to their poor ability to recognize each amino acid within the N-terminal half.

Induction of CTL line and clones specific for L-valine or D-valine at position 325 within P18-I10

Then, to study the detailed molecular interactions in determining T-cell specificity, we attempted to generate a CTL line specific for I10(325v) having a single D-type amino acid substitution in P18-I10 at position 325 using immunization of BALB/c mice with syngeneic splenic dendritic cells pulsed with the peptide (23). The I10(325v)-specific CTL line, LINE-IIIB(325D), was successfully established. Although LINE-IIIB(325D) showed some cross-reactivity to P18-I10 in a dose-dependent manner, it was highly specific for I10(325v) (Fig. 3 *A*). Similarly, LINE-IIIB had some cross-reactivity to I10(325v)-sensitized targets (Fig. 3 *B*).

Using limiting dilution techniques described elsewhere (17), we successfully established two clones, IIE11(D) and IIA4(D), predominantly specific for I10(325v) but not for P18-I10 from LINE-IIIB(325D) cells (Fig. 3 *C*) as well as two P18-I10-specific CTL clones, IIH7(L) and IB9(L), from the LINE-IIIB cells (Fig. 3 *D*). Thus, we had established four highly specific clones, two of which were specific for the D-type of valine (v), and the other two for the L-type of valine (V) at position 325 within P18-I10.

Specificity and characterization of the established CTL clones

We further examined the fine specificities of the CTL clones using a series of substituted peptides, each with a single amino acid substitution of either the L- or D-type having an aliphatic or aromatic structure at position 325 in P18-I10 (Table 1).

Among the D-specific clones, IIE11(D) did not cross-react with I10(325I) at all and was strictly specific for the D-type

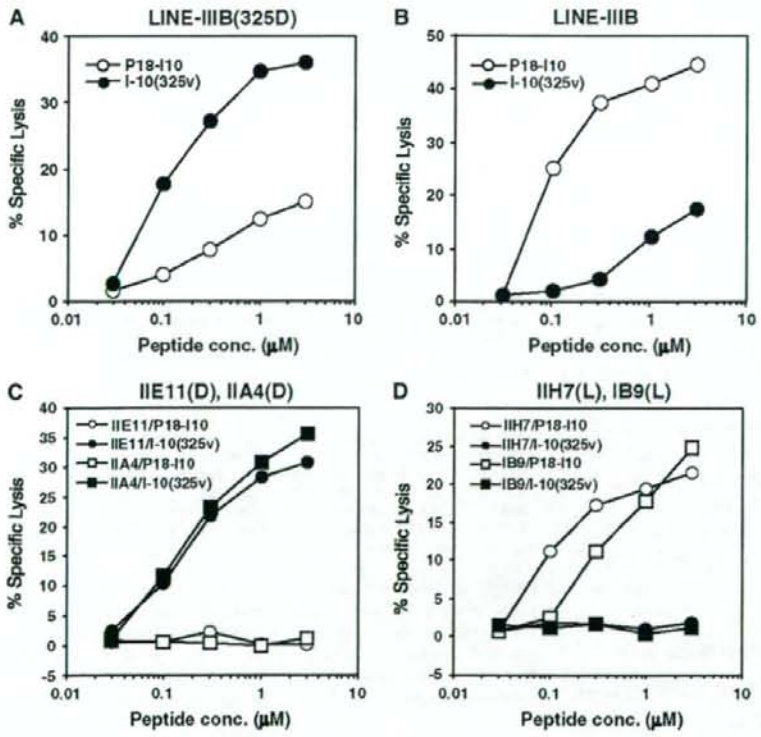

FIGURE 3 Comparison of specificity of the newly established CTL lines and clones against two peptides, peptide P18-I10 and I10(325v). We examined the cytolytic activity of the following distinct CTL lines and clones using a 5-h ^{51}Cr-release assay. To test the peptide specificity, effector cells and ^{51}Cr-labeled BALB/c.3T3 fibroblast targets (E/T ratio was 10:1) were incubated in the presence of various concentrations of either P18-I10 or I10(325v). (*A*) LINE-IIIB(325D) specific for I10(325v) was used for effector cells. (*B*) LINE-IIIB specific for P18-I10 was used for effector cells. (*C*) The CTL clones, IIE11(D) and IIA4(D), derived from LINE-IIIB(325D) were used as effector cells. (*D*) The CTL clones, IIH7(L) and IB9(L), from LINE-IIIB were used as effector cells. Standard errors of the means of triplicate cultures were <5% of the mean in each case. Each experiment was performed at least three times.

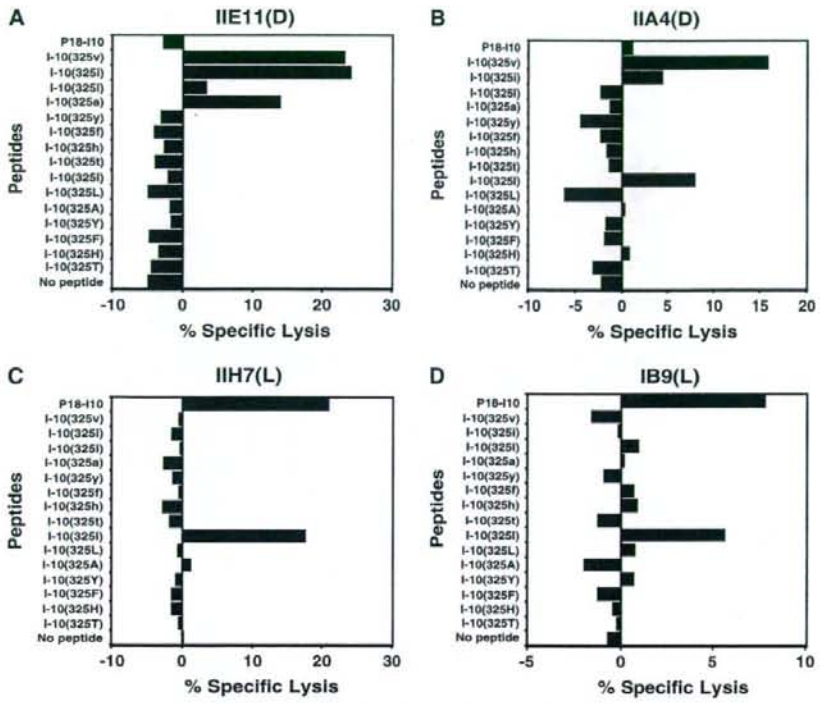

FIGURE 4 Effects of a single amino acid substitution at position 325 within P18-I10 on target sensitization for CTL recognition. We measured the cytolytic activity of the CTL lines and clones using a 5-h ^{51}Cr-release assay. For the analysis of fine peptide specificity, effector cells and ^{51}Cr-labeled BALB/c.3T3 fibroblast targets were mixed with 10 μM of each substituted peptide. The following four clones were used as effectors (E/T ratio was 20:1): (*A*) clone IIE11(D), (*B*) clone IIA4(D), (*C*) clone IIH7(L), and (*D*) clone IB9(L). Standard errors of the means of triplicate cultures were <5% of the mean in each case. Each experiment was performed at least three times.

substitution such as I10(325i) and I10(325a) as well as for the original I10(325v) (Fig. 4 *A*), whereas IIA4(D) showed a weak cross-reactivity for both types of isoleucine, I10(325I) and I10(325i), as well as for the original I10(325v) (Fig. 4 *B*). In addition, both of the L-type-specific CTL clones, IIH7(L) and IB9(L), cross-reacted with I10(325I) as well as with the original P18-I10 (Fig. 4, *C* and *D*). These findings indicate that the CTL clones can specifically distinguish the optical isomers at position 325.

Because P18-I10-specific CTL and their clones are CD8$^+$, D^d-class I MHC molecule-restricted conventional $\alpha\beta$T lymphocytes, we next confirmed the surface molecules and MHC-restriction of the I10(325v)-specific line and clones. LINE-IIIB(325D) and two clones, IIE11(D) and IIA4(D), were all CD3$^+$, CD4$^-$, CD8$^+$, and TCR$\alpha\beta^+$ by FACS analysis (data not shown), and they did not show any cytotoxicity against NK-sensitive YAC-1 cells (data not shown). Moreover, using three L cell (H-2^k) transfectants expressing the class I MHC of the d-haplotype, T4.8.3 (D^d), T1.1.1 (L^d), and B4III2 (K^d) (25,26), we confirmed that the I10(325v)-specific CTL line and clones were restricted by the D^d class I MHC molecule (data not shown).

TCR-sequences of the established clones

Taken together, the two groups of CTL clones with high specificity to the substituted P18-I10-derived peptides, having either the L-type of valine (V) or D-type of valine (v) at position 325, expressed both CD8 and $\alpha\beta$ TCRs, and were restricted by the same class I MHC molecule, D^d. Therefore, taking advantage of the unique combinations of CTL clones, we attempted to perform a precise analysis of the interaction between the TCRs of those clones and the amino acid at

	TCRα chain			
CTL clones	Vα	N	Jα	
IIE11(D)	CAMR	EAD	SNYQLIWGSGTKLIIKPD	Vα16-Jα18BBM142
IIA4(D)	CAMR	EAD	SNYQLIWGSGTKLIIKPD	Vα16-Jα18BBM142
IIH7(L)	CALS	ED	SNYQLIWGSGTKLIIKPD	Vα3-Jα18BBM142
IB9(L)	CAAS	D	SNYQLIWGSGTKLIIKPD	Vα2-Jα18BBM142

	TCRβ chain			
CTL clones	Vβ	N-D-N	Jβ	
IIE11(D)	CASS	DWGGS	TGQLYFGEGSKLTVL	Vβ8.3-Jβ2.2
IIA4(D)	CASS	DWGGS	TGQLYFGEGSKLTVL	Vβ8.3-Jβ2.2
IIH7(L)	CASS	LGYT	EVFFGKGTRLTVV	Vβ7-Jβ1.1
IB9(L)	CASS	LGVT	EVFFGKGTRLTVV	Vβ7-Jβ1.1

FIGURE 5 Nucleotide and amino acid sequences that form the V(D)J region of the TCRα and -β chain from the established CTL clones. We analyzed the amino acid sequences of TCRs in two groups of CTL clones with high specificity to substituted P18-I10-derived peptides, having either the D-type of valine (v) (IIE11(D) and IIA4(D)) or the L-type of valine (V) at position 325 (IIH7(L) and IB9(L)) restricted by the same class I MHC molecules, D^d.

position 325 within epitope to determine the specificity by comparing their TCR sequences.

To investigate the actual amino acid sequences of the TCRs in the CTL clones, we extracted their mRNA and analyzed the nucleotide sequences of the α- and β-chain transcripts after a cDNA synthesis and PCR amplifications. The Vα usage of the I10(325v)-specific clones, IIE11(D) and IIA4(D), were both Vα16 (36), whereas that of the P18-I10-specific clones, IIH7(L) and IB9(L), were Vα3 (37) and Vα2 (BLASTN Accession U88296), respectively (Fig. 5). It should be noted that all of the four distinct clones used the same uncommon Jα gene segment, 18BBM142, determined from a murine alloreactive T-cell hybridoma specific for I-A^{bm12} (38). In contrast, the Vβ usage of the 325(v)-specific clones, IIE11(D) and IIA4(D), was Vβ8.3 (39) with the Jβ 2.2 segment (40) bearing the same CDR3, "DWGGS," whereas the Vβ usage of the 325(L)-specific clones, IIH7 and IB9, was Vβ7 with the Jβ1.1 segment (41) encoding a distinct sequence, "LGYT" and "LGVT," respectively, in the CDR3 flap (Fig. 5). These results strongly indicate that the TCRβ chains of those clones may be responsible for the specificity of the epitope.

Identification of the interaction site between the TCRs and a critical amino acid at position 325 to determine epitope specificity by molecular modeling analysis

Based on the above findings, we then studied the site that determines the epitope specificity of the TCRβ chain in the CTL clones using a 3D molecular modeling analysis (see Materials and Methods). We used the LIBRA software (29,42) to select five compatible templates with excellent Standardized Scores (SD value) for both Vβ7 and Vβ8.3 (Fig. 6 *A*). Fig. 6 *B* shows the alignment of the five most suitable templates for each TCR.

We then used the MODELLER software (30,31,33) to model the 3D structure of the TCR. First, to confirm the

A

Vβ7

Rk	StrC	Lsr	Lal	Rsc	SD	Rs/N	ID%
1	1a6wH	120	127	-65.6	-4.24	-0.517	22.0
2	1dn0D	217	131	-60.1	-3.73	-0.459	19.1
3	1tcrA	202	128	-58.7	-3.60	-0.459	21.1
4	1ao7D	115	124	-56.6	-3.40	-0.457	15.3
5	1kb5A	115	122	-56.4	-3.38	-0.462	23.0

Vβ8.3

Rk	StrC	Lsr	Lal	Rsc	SD	Rs/N	ID%
1	1hxmB	230	118	-58.1	-4.24	-0.492	13.6
2	1etzB	228	124	-55.4	-3.97	-0.446	12.9
3	1fo0A	114	116	-54.5	-3.88	-0.470	19.0
4	1h5bA	113	118	-53.5	-3.78	-0.453	25.4
5	1d1fL	108	114	-52.6	-3.69	-0.461	19.3

B

FIGURE 6 (*A*) Compatible templates with excellent Standardized Scores (SD value) for both Vβ7 and Vβ8.3 selected from the LIBRA software. Bold abbreviations are defined as follows: Rk, rank position; StrC, structural code of PDB (the last character is a subunit name); Lsr, length of the structural template; Lal, length of the aligned region; Rsc, raw score of the structural template; SD, standardized score; Rs/N, raw score (Rsc) normalized by the alignment length (Lal); ID%, sequence identity. (*B*) Sequence alignment of TCR Vβ7, Vβ8.3, and each of the five template proteins (1a6wH, 1dn0D, 1tcrA, 1ao7D, 1kb5A for Vβ7 and 1hxmB, 1etzB, 1fo0A, 1h5bA, 1d1fL for Vβ8.3) obtained from the LIBRA software. In this figure, the amino acid sequences of CDR1 and CDR3 from TCR Vβ7 or Vβ8.3 are drawn in red and green, respectively. In 10 template proteins, the corresponding portion of the CDR1 and CDR3 regions are also drawn in red and green, respectively. Conserved cysteine residues upstream of CDR1 and CDR3 are drawn in magenta. Two or three amino acids between the conserved cysteine residues and CDR1 are drawn in blue (see Discussion).

accuracy of our molecular modeling method, we predicted the 3D structure of a previously analyzed protein using MODELLER and then compared it with the experimental 3D structure obtained from x-ray crystallographic analysis for the same protein. We selected two proteins (PDB cord 1dn0D and 1a6wH) having high scores in Fig. 6 *A* and then calculated the 3D structure of 1dn0D using 1a6wH as a template. As shown in Fig. 7, the 3D structure of 1dn0D obtained from MODELLER was similar to that obtained experimentally, and their core regions were nearly identical. These results suggest that our molecular modeling method could be useful for the structural analysis of unknown TCRs.

We next predicted the 3D structures of TCR Vβ7 and Vβ8.3 and analyzed their interactions with P18-I10. The obtained 3D structures for Vβ7 using the five selected templates were quite similar (Fig. 8, *A–D*) and could be confirmed by rotating the calculated structures from various angles (data not shown). In addition, each obtained 3D structure for Vβ7 was fitted to the TCRβ part in 1kj2 to analyze the interaction with the P18-I10 peptide. Although both the CDR1 (*blue*) and CDR3 (*red*) in Vβ7 appeared to interact with the C-terminal half of P18-I10, the critical site for determining epitope specificity (325V, *bright green*) within P18-I10 was found to be more closely associated with the canonical free bottom portion of CDR1 and not with the CDR3 loop (Fig. 8, *A* and *B*): the CDR3 loop is too far from 325V. However, when the 325V was substituted with 325v (*bright red*), the CDR1 loop of Vβ7 might come in contact with the 325v (Fig. 8, *C* and *D*), which seemed to induce conformational interference between the TCR and I10(325v), and thus, the H-2D^d-restricted peptide I10(325v) would not be recognized by the P18-I10-specific clones, IIH7(L) and IB9(L). These results are consistent with our experimental results and indicate that the CDR1 loop of TCR Vβ7 should be the key site for determining P18-I10 specificity in the interaction with the L-valine at position 325.

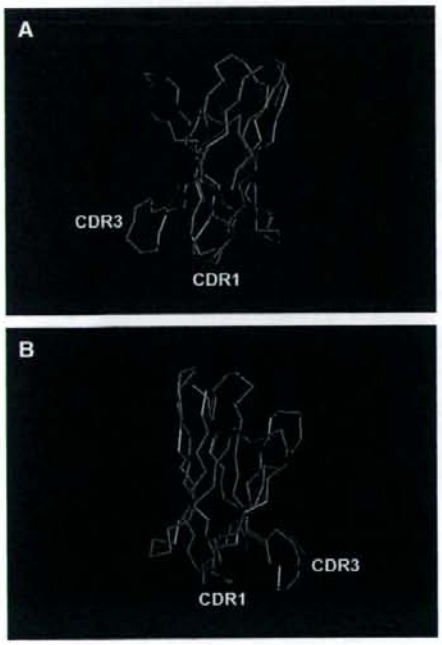

FIGURE 7 Comparison between the predicted 3D structure for 1dn0D by the MODELLER software and that of the same protein registered in PDB. The 3D structure of the protein (PDB cord 1dn0D) was predicted by the MODELLER, a molecular modeling software, using a protein (e.g., PDB cord 1a6wH) as a template. The predicted 3D structure for 1dn0D is drawn in blue, and the PDB 3D structure is drawn in red. Their backbone representations in the molecular modeling are drawn from rotated two distinct views (*A* and *B*).

Similarly, the molecular modeling for Vβ8.3 was performed using another five of the most suitable templates shown in Fig. 6 *A*; each of these actual sequences is shown in Fig. 6 *B*. The calculated 3D structures of Vβ8.3 based on the five templates had almost the same features (Fig. 8, *E–H*) as seen in the case of Vβ7. In contrast to the case of Vβ7, 325v (*bright red*) seemed to be associated with the free bottom portion of the CDR1 loop of Vβ8.3 but not with the CDR3 loop of Vβ8.3 (Fig. 8, *E* and *F*). However, the distance between the 325V (*bright green*) and the CDR1 loop in the case of Vβ8.3 appeared to be greater than that in the case of Vβ7 (Fig. 8, *G* and *H*), which can make a good contact with the 325V in P18-I10.

To substantiate the interaction between valine at position 325 and TCR-CDR1, the distance between terminal atoms in the side chain of amino acids within the epitope peptide and atoms in the main chain of the nearest portion within the TCR was calculated. As shown in Table 2, first to confirm the reliability of our molecular modeling, the distance between the two terminal atoms (OD1 and OD2) in the side chain of the seventh amino acid, aspaltic acid (D), within epitope peptide pKB1(aa: KVITFIDL) and the nearest portion in the TCR from OD1 or OD2 was determined using an already reported TCR/peptide/MHC complex, 1kj2 (PDBcode) obtained from x-ray crystallographic analysis (5). Based on the above observation, the distance between the two terminal atoms (CG1 and CG2) in the side chain of 325V or 325v and their surrounding atoms in the main chain of the obtained TCRs, Vβ7 and Vβ8.3, calculated (Tables 3 and 4) and compared with that of 1kj2. The results indicate that the distance between 325V and CDR1 in Vβ7 is similar to the distance in the case of 1kj2, whereas the distance between 325v and CDR1 in Vβ7 is too small, which may induce conformational interference between them. In contrast, the distance between 325v and CDR1 in Vβ8.3 is similar to 1kj2, but the distance between the 325V and the CDR1 in Vβ8.3 appeared to be too far from that of 1kj2. These results again agreed with our experimental results that Vβ8.3 recognized the epitope I10(325v) having D-valine at position 325 via CDR1 but did not recognize the P18-I10 containing L-valine at that position.

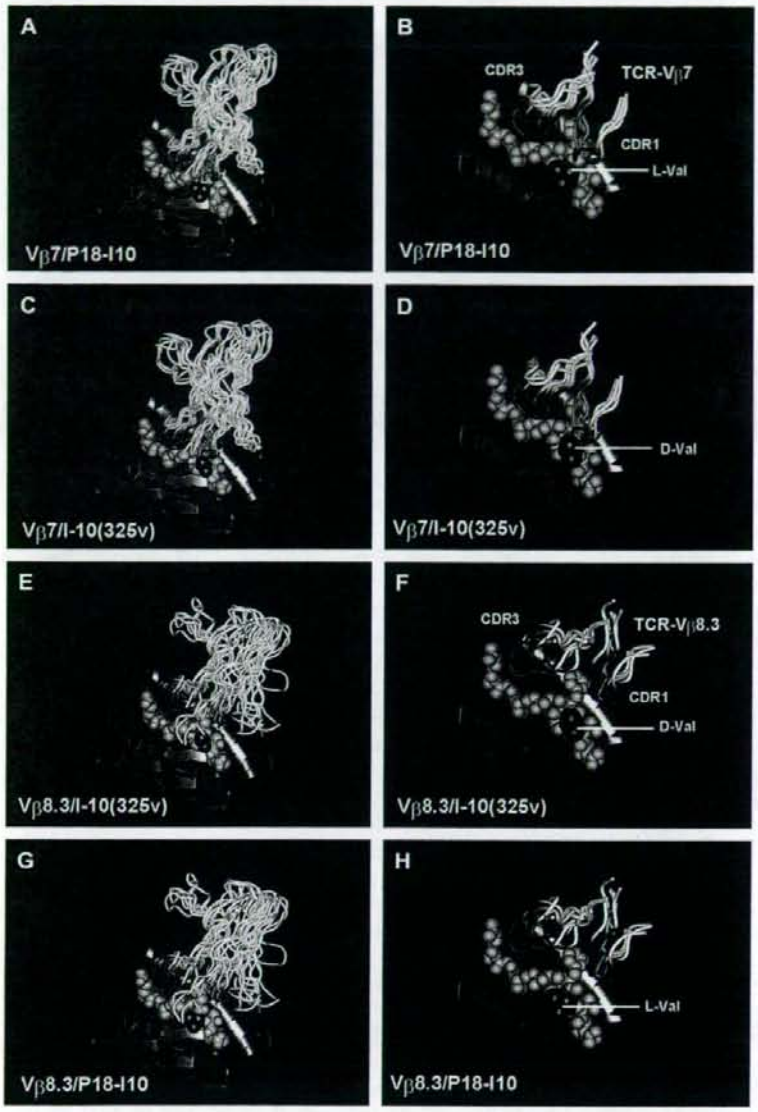

FIGURE 8 3D structures representing the interaction between TCR Vβ7 (Vβ8.3) and P18-I10/H-2D^d Complex or the interaction between TCR Vβ7 (Vβ8.3) and I10(325v)/H-2D^d complex. (*A–H*) The ternary complex of TCR Vβ7 or Vβ8.3 onto either P18-I10 or I10(325v) bounded to the H-2D^d class I MHC molecules were illustrated by computer-based molecular modeling (see Materials and Methods). Horizontal gray backbone represents the H-2D^d class I MHC molecule, and the yellow ball format indicates the D^d-bounded epitope peptide P18-I10. Vertical overlapping white backbones indicate either TCR Vβ7 or Vβ8.3. In these figures, Vβ7 and Vβ8.3 made from five distinct template proteins were overlaid in one figure. The CDR1 and CDR3 loops from both TCR Vβ chains are drawn in cyan and red, respectively. The L-type of valine (V) and the D-type of valine (v) at position 325, where epitope specificity appears to be determined, are shown in bright green and bright red, respectively. The 3D-structures of the (*A*) Vβ7 /H-2D^d/P18-I10, (*B*) enlarged figure of *A*, (*C*) Vβ7 /H-2D^d/I10(325v), (*D*) enlarged figure of *C*, (*E*) Vβ8.3 /H-2D^d/I10(325v), (*F*) enlarged figure of *E*, (*G*) Vβ8.3/H-2D^d/P18-I10, and (*H*) enlarged figure of *G* are shown in eight independent panels.

Therefore, CDR1, but not the CDR3 loop, in Vβ7 or Vβ8.3 seems to play an important role in the recognition of each specific epitope peptide. Moreover, amino acids at positions 26 to 31: DMSHET within the CDR1 of Vβ7, or TNSHNY within the CDR1 of Vβ8.3, appear to interact with the critical amino acid at position 325 to determine the epitope specificity.

DISCUSSION

In our previous study, we found that the amino acids at positions 322R and 324F were critical for D^d binding, and those at position 325V were essential for interacting with TCRs (8,17). Also, the C-terminus 327I appears to be a key amino acid for D^d binding to form the D^d-binding motif (8,18). In this study, we demonstrated that the substitution of a positively charged 322R by 322r did not result in measurable changes in target sensitization, although in our previous study the substitution with uncharged alanine (A) completely eliminated the capacity to sensitize the targets (17), indicating that a positive electric charge must be critical for D^d binding at position 322, and that a reduction of charge in the amino acid might diminish the epitope potency for T-cell activation. As shown in Fig. 1 *B*, the side chains of V and T have the same 3D

TABLE 2 The distance between two terminal atoms in the side chain of the seventh amino acid, Asp (D) within epitope peptide and atoms in main chain of the nearest portion within the TCR

	N (S28)	C_a (S28)	C (S28)	O (S28)	N (Q29)	C_a (Q29)	C (Q29)	O (Q29)	N (Y30)	C_a (Y30)	C (Y30)	O (Y30)
OD1	10.86	9.55	8.37	7.24	8.76	7.98	7.60	6.99	8.27	8.39	8.29	9.37
OD2	8.83	7.48	6.40	5.24	6.97	6.44	6.21	5.91	6.76	7.08	6.84	7.88

Unit of the distance is Å. The values are calculated using 1kj2 (PDB code), which is TCR/peptide/ MHC complex structure obtained from x-ray crystallographic analysis. The OD1 or OD2 represents the terminal atom of the side chain in the seventh amino acid, aspaltic acid (D), within epitope peptide pKB1(aa: KVITFIDL). The amino acids Ser 28 (S28), Gln 29 (Q29), and Tyr 30 (Y30) are the nearest portion within the TCR from the OD1 or OD2.

structure, except for the hydrogen atoms, if one terminal carbon atom of the side chain of V is exchanged for one oxygen atom. According to the quantum chemical calculation, the net charge of the carbon or the oxygen is −0.3e or −0.4e, respectively. In addition, three hydrogen atoms, which have positive charges, are added to the carbon, whereas one hydrogen atom is added to the oxygen. Thus, T generates a greater negative net charge than V. The influence of this charge difference was evident when LINE-IIIB recognized the peptide. It is likely that T had a greater repulsive force against the oxygen atoms in the CDR1 loop compared with V. This repulsive force may account for the significant reduction in the recognition by LINE-IIIB after substitution with T. These findings indicate that the charge of an amino acid at a specific position within an epitope can affect its binding capacity to MHC molecules and/or the interaction with a TCR.

Although the method we applied here for modeling the TCR/peptide/class I MHC complex was not directly based on crystallographic analysis, our computer-based molecular modeling was still accurate. Indeed, as demonstrated in Fig. 7, the predicted 3D structure for 1dn0D by MODELLER was similar to that determined experimentally, and the core regions appeared to be nearly identical. This reflects the fact that the 3D structures of the core regions of the TCR consist of a four-stranded antiparallel β-sheet and a three-stranded anti-parallel β-sheet linked by a disulfide bond. Although the predicted 3D structure of CDR3 seems slightly different from the experimental 3D structure of CDR3 because of the large loop, the predicted 3D structure of CDR1 appears almost the same as the experimental 3D structure. These results suggest that the TCR domain predicted by the present molecular modeling methods can become useful and reliable tools for the structural analysis of TCRs.

TABLE 3 The distance between two terminal atoms in the side chain of 325V or 325v and atoms in main chain of the obtained TCR-CDR1 through molecular modeling

	Vβ7	N(S)	Cα(S)	C(S)	O(S)	N(H)	Cα(H)	C(H)	O(H)
1a6wH	CG1(325V)	10.20	9.55	8.56	8.52	7.99	7.08	7.85	7.48
	CG2(325V)	9.57	8.88	7.62	7.41	7.01	5.80	6.17	5.57
1dn0D	CG1(325V)	10.03	9.43	8.73	8.11	9.12	8.90	9.30	9.33
	CG2(325V)	9.40	8.79	7.77	6.99	8.06	7.58	7.65	7.48
1tcrA	CG1(325V)	7.69	6.38	6.49	7.45	5.86	6.44	7.84	8.34
	CG2(325V)	6.63	5.41	5.09	5.76	4.51	4.80	6.29	6.97
1ao7D	CG1(325V)	7.57	6.48	7.18	6.85	8.40	9.21	9.59	10.11
	CG2(325V)	6.91	5.63	5.85	5.34	6.96	7.48	7.89	8.63
1kb5A	CG1(325V)	7.51	8.02	7.58	6.44	8.67	8.81	9.71	10.44
	CG2(325V)	6.77	7.06	6.21	4.99	7.08	6.92	7.89	8.79
1a6wH	CG1(325v)	8.10	7.48	6.70	6.85	6.20	5.60	6.69	6.63
	CG2(325v)	6.95	6.27	5.12	5.09	4.53	3.56	4.38	4.18
1dn0D	CG1(325v)	7.94	7.34	6.88	6.41	7.39	7.47	8.10	8.42
	CG2(325v)	6.79	6.16	5.28	4.59	5.73	5.59	5.91	6.14
1tcrA	CG1(325v)	6.51	5.12	5.35	6.50	4.59	5.40	6.57	6.84
	CG2(325v)	5.01	3.61	3.26	4.28	2.35	3.02	4.34	4.78
1ao7D	CG1(325v)	5.64	4.73	5.73	5.63	6.98	8.02	8.36	8.66
	CG2(325v)	4.39	3.09	3.63	3.36	4.88	5.73	6.12	6.61
1kb5A	CG1(325v)	5.60	6.21	6.12	5.18	7.37	7.86	8.74	9.24
	CG2(325v)	4.21	4.55	4.02	2.91	5.16	5.49	6.49	7.13

Unit of the distance is Å. The code 1a6wH, 1dn0D, 1tcrA, 1ao7D, or 1kb5A represents each template protein to determine the structure of Vβ7. CG1 and CG2 are two terminal atoms of side chain in 325V or 325v. The successive two amino acids, Ser and His, within CDR1 of Vβ7 are the nearest portion for CG1 or CG2.

In these sorts of structural analyses, it should be acknowledged that a substitution of D-valine (v) for L-valine (V) would result in a conformational interference between the class I MHC molecule and the D-valine (v), which itself could decrease the recognition response by LINE-IIIB. However, as shown in Fig. 9, no conformational interference occurred in this study. Thus, I10(325v) would also be associated with the class I MHC molecule so that TCRs may recognize the epitope. Therefore, our findings suggest that the change in the recognition response by LINE-IIIB after the D-valine (v) substitution reflects the interaction with the TCR.

Our molecular modeling analysis demonstrated that the critical area of the TCR for interacting with 325V within P18-I10 was the peptide DMSHET, within the CDR1 of Vβ7. In contrast, the substituted peptide with the D-type amino acid, I10(325v), was recognized by the peptide TNSHNY within the CDR1 of Vβ8.3. Therefore, the CDR1 in the Vβ7 or Vβ8.3 might play an important role in recognizing the epitope P18-I10 or I10(325v), respectively, and, in particular, the distance between CDR1 and the amino acid 325V or 325v within the peptide seemed to be essential for recognizing the epitope. Taken together, the results derived from our molecular modeling strategy appear to be consistent with the experimental results.

Although the epitope specificity created by TCRs has been reported to be dependent mainly on the amino acid sequences in the CDR3 regions for both the TCRα and β chains (43,44), crystallographic analyses on various TCR and peptide/MHC interactions have suggested that both the CDR1 and CDR3 in

TABLE 4 The distance between two terminal atoms in the side chain of 325V or 325v and atoms in main chain of the obtained TCR-CDR1 through molecular modeling

Vβ8.3	N(T)	Cα(T)	C(T)	O(T)	N(N)	Cα(N)	C(N)	O(N)	N(S)	Cα(S)	C(S)	O(S)
1hxmBCG1(325V)	13.34	12.22	11.94	12.32	11.47	11.47	10.62	9.61	11.19	10.74	11.80	12.32
CG2(325V)	12.54	11.59	11.25	11.41	11.00	10.98	9.90	8.83	10.34	9.64	10.65	11.36
1etzBCG1(325V)	13.77	13.45	12.19	11.26	12.24	11.31	9.99	8.95	10.16	9.20	9.41	10.25
CG2(325V)	13.14	12.75	11.63	10.76	11.76	11.02	9.57	8.73	9.41	8.22	8.32	9.30
1fo0ACG1(325V)	10.43	9.82	9.37	9.20	9.43	9.34	10.58	11.43	10.85	12.07	13.27	13.89
CG2(325V)	9.41	8.58	8.29	8.45	8.18	8.25	9.66	10.47	10.12	11.47	12.47	13.09
1h5bACG1(325V)	11.98	10.99	10.34	10.13	10.23	9.81	10.97	12.02	10.95	12.14	12.24	11.29
CG2(325V)	11.18	10.43	9.87	9.95	9.52	9.16	10.18	11.13	10.20	11.29	11.10	10.02
1dlfLCG1(325V)	12.46	11.35	10.28	9.72	10.18	9.27	10.19	11.40	9.77	10.82	11.61	11.18
CG2(325V)	11.39	10.46	9.42	9.14	9.06	8.14	9.06	10.25	8.69	9.75	10.28	9.64
1hxmBCG1(325v)	11.19	10.04	9.53	9.84	8.98	8.81	7.89	6.96	8.39	7.95	9.00	9.47
CG2(325v)	10.21	9.16	8.72	8.95	8.37	8.32	7.31	6.25	7.84	7.33	8.47	9.12
1etzBCG1(325v)	11.63	11.33	10.01	9.08	10.05	9.08	7.83	6.75	8.15	7.37	7.76	8.53
CG2(325v)	10.57	10.17	9.00	8.11	9.13	8.38	6.95	6.11	6.87	5.78	6.11	7.09
1fo0ACG1(325v)	8.55	8.16	7.68	7.31	7.99	7.98	9.10	9.82	9.44	10.57	11.78	12.26
CG2(325v)	6.96	6.31	6.03	6.03	6.22	6.47	7.78	8.44	8.38	9.66	10.67	11.12
1h5bACG1(325v)	9.98	8.91	8.17	7.84	8.17	7.74	8.99	10.05	9.05	10.33	10.63	9.80
CG2(325v)	8.70	7.89	7.22	7.27	6.92	6.57	7.69	8.66	7.83	9.04	9.03	8.07
1dlfLCG1(325v)	10.66	9.50	8.36	7.65	8.40	7.51	8.42	9.61	8.05	9.15	10.11	9.84
CG2(325v)	9.11	8.13	6.97	6.57	6.70	5.75	6.71	7.91	6.41	7.59	8.30	7.82

Unit of the distance is Å. The code 1hxmB, 1etzB, 1fo0A, 1h5bA, or 1dlfL represents each template protein to determine the structure of Vβ8.3. CG1 and CG2 are two terminal atoms of side chain in 325V or 325v. The successive three amino acids, Thr, Asn, and Ser, within CDR1 of Vβ8.3 are the nearest portion for CG1 or CG2.

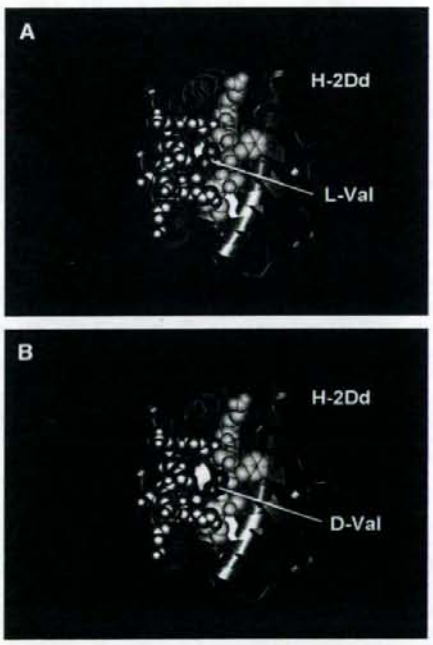

FIGURE 9 (*A* and *B*) 3D structures of P18-I10/H-2D^d complex and I10(325v)/H-2D^d complex. Gray ribbon and ball format represent the H-2D^d class I MHC molecule, and the yellow ball format indicates the D^d-bounded epitope peptide, P18-I10 or I10(325v). In the H-2D^d class I MHC molecule, only the positions for interaction with 325V are drawn in the ball format, for clarity. The L-type of valine (V) and the D-type of valine (v) at position 325 are shown in green and red, respectively. Radius of ball format indicates van der Waals radius.

the TCRα and TCRβ chains might contact with the antigenic peptide/MHC complex (1,2,5,6), particularly with the carboxyl-terminal portion of the peptides (2). Moreover, recent reports have shown that the CDR1 in Vβ10 participated in class I MHC molecule-mediated T-cell recognition (45,46). In these reports, significant alteration in the capacity to bind class I MHC molecules and in the ability to respond to the peptide/MHC complex was demonstrated when a single amino acid substitution was introduced into the CDR1 of TCR Vβ10 by site-directed mutagenesis. Indeed, we have shown here that the CDR1 in the TCRβ chains appeared to interact directly with the key amino acid for determining epitope specificity. Thus, if the most critical amino acid for determining the epitope specificity is located near the C-terminal portion of a peptide such as P18-I10, not only the CDR3 but also the CDR1 in the TCRβ chain may be involved in determining antigen specificity.

It is also important to consider the role of the primary structures in TCR recognition. As demonstrated in Fig. 6 *B*, there are two cysteine (C) residues positioned upstream of CDR1 (*magenta*) and CDR3 (*magenta*) of both TCR Vβ7 and Vβ8.3. These residues bind each other via a disulfide bond and must be a basic structure of TCRs because they are conserved in most of the murine TCR sequences (47) . The two or three amino acids (*blue*) between the conserved cysteine (C) residues and the CDR1 would be key amino acids in forming the 3D structure of CDR1, although they do not interact directly with the epitope peptide. If only these amino acids are exchanged for other amino acids, the 3D structure of CDR1 affecting the recognition of an amino acid at position 325 would change. Indeed, these amino acids are

highly variable for both TCR Vβ7 and Vβ8.3 (Fig. 6 *B*) and for various other murine TCR sequences (47), whereas the regions just after CDR1 are mostly conserved. These amino acids are likely to participate in the peptide recognition by creating small changes in the 3D structure of CDR1. In this regard, both CDR1 and the two or three amino acids between the cysteine (C) and CDR1 may play a important role in recognizing position 325 within P18-I10 or I10(325v).

We thank Dr. Megumi Takahashi for her assistance with the DNA sequence analysis of the TCRs.

This work was supported in part by grants from the Ministry of Education, Science, Sport, and Culture, from the Ministry of Health and Labor and Welfare, Japan; from the Japanese Health Sciences Foundation; and from and by the Promotion and Mutual Aid Corporation for Private Schools of Japan.

REFERENCES

1. Garboczi, D. N., P. Ghosh, U. Utz, Q. R. Fan, W. E. Biddison, and D. C. Wiley. 1996. Structure of the complex between human T-cell receptor, viral peptide and HLA-A2. *Nature*. 384:134–141.
2. Garcia, K. C., M. Degano, R. L. Stanfield, A. Brunmark, M. R. Jackson, P. A. Peterson, L. Teyton, and I. A. Wilson. 1996. An alphabeta T cell receptor structure at 2.5 A and its orientation in the TCR-MHC complex. *Science*. 274:209–219.
3. Garboczi, D. N., and W. E. Biddison. 1999. Shapes of MHC restriction. *Immunity*. 10:1–7.
4. Hennecke, J., and D. C. Wiley. 2001. T cell receptor-MHC interactions up close. *Cell*. 104:1–4.
5. Reiser, J. B., C. Gregoire, C. Darnault, T. Mosser, A. Guimezanes, A. M. Schmitt-Verhulst, J. C. Fontecilla-Camps, G. Mazza, B. Malissen, and D. Housset. 2002. A T cell receptor CDR3beta loop undergoes conformational changes of unprecedented magnitude upon binding to a peptide/MHC class I complex. *Immunity*. 16:345–354.
6. Garcia, K. C., M. Degano, L. R. Pease, M. Huang, P. A. Peterson, L. Teyton, and I. A. Wilson. 1998. Structural basis of plasticity in T cell receptor recognition of a self peptide-MHC antigen. *Science*. 279: 1166–1172.
7. Takahashi, H., J. Cohen, A. Hosmalin, K. B. Cease, R. Houghten, J. L. Cornette, C. DeLisi, B. Moss, R. N. Germain, and J. A. Berzofsky. 1988. An immunodominant epitope of the human immunodeficiency virus envelope glycoprotein gp160 recognized by class I major histocompatibility complex molecule-restricted murine cytotoxic T lymphocytes. *Proc. Natl. Acad. Sci. USA*. 85:3105–3109.
8. Takeshita, T., H. Takahashi, S. Kozlowski, J. D. Ahlers, C. D. Pendleton, R. L. Moore, Y. Nakagawa, K. Yokomuro, B. S. Fox, and D. H. Margulies. 1995. Molecular analysis of the same HIV peptide functionally binding to both a class I and a class II MHC molecule. *J. Immunol*. 154:1973–1986.
9. Takahashi, H., S. Merli, S. D. Putney, R. Houghten, B. Moss, R. N. Germain, and J. A. Berzofsky. 1989. A single amino acid interchange yields reciprocal CTL specificities for HIV-1 gp160. *Science*. 246: 118–121.
10. Takahashi, H., Y. Nakagawa, C. D. Pendleton, R. A. Houghten, K. Yokomuro, R. N. Germain, and J. A. Berzofsky. 1992. Induction of broadly cross-reactive cytotoxic T cells recognizing an HIV-1 envelope determinant. *Science*. 255:333–336.
11. Shirai, M., C. D. Pendleton, and J. A. Berzofsky. 1992. Broad recognition of cytotoxic T cell epitopes from the HIV-1 envelope protein with multiple class I histocompatibility molecules. *J. Immunol*. 148: 1657–1667.
12. Palker, T. J., M. E. Clark, A. J. Langlois, T. J. Matthews, K. J. Weinhold, R. R. Randall, D. P. Bolognesi, and B. F. Haynes. 1988. Type-specific neutralization of the human immunodeficiency virus with antibodies to env-encoded synthetic peptides. *Proc. Natl. Acad. Sci. USA*. 85:1932–1936.
13. Rusche, J. R., K. Javaherian, C. McDanal, J. Petro, D. L. Lynn, R. Grimaila, A. Langlois, R. C. Gallo, L. O. Arthur, P. J. Fischinger, D. P. Bolognesi, S. D. Putney, and T. J. Matthews 1988. Antibodies that inhibit fusion of human immunodeficiency virus-infected cells bind a 24-amino acid sequence of the viral envelope, gp120. *Proc. Natl. Acad. Sci. USA*. 85:3198–3202.
14. Goudsmit, J., C. Debouck, R. H. Meloen, L. Smit, M. Bakker, D. M. Asher, A. V. Wolff, C. J. Gibbs, Jr., and D. C. Gajdusek. 1988. Human immunodeficiency virus type 1 neutralization epitope with conserved architecture elicits early type-specific antibodies in experimentally infected chimpanzees. *Proc. Natl. Acad. Sci. USA*. 85:4478–4482.
15. Takahashi, H., R. N. Germain, B. Moss, and J. A. Berzofsky. 1990. An immunodominant class I-restricted cytotoxic T lymphocyte determinant of human immunodeficiency virus type 1 induces CD4 class II-restricted help for itself. *J. Exp. Med*. 171:571–576.
16. Clerici, M., D. R. Lucey, R. A. Zajac, R. N. Boswell, H. M. Gebel, H. Takahashi, J. A. Berzofsky, and G. M. Shearer. 1991. Detection of cytotoxic T lymphocytes specific for synthetic peptides of gp160 in HIV-seropositive individuals. *J. Immunol*. 146:2214–2219.
17. Takahashi, H., R. Houghten, S. D. Putney, D. H. Margulies, B. Moss, R. N. Germain, and J. A. Berzofsky. 1989. Structural requirements for class I MHC molecule-mediated antigen presentation and cytotoxic T cell recognition of an immunodominant determinant of the human immunodeficiency virus envelope protein. *J. Exp. Med*. 170:2023–2035.
18. Corr, M., L. F. Boyd, E. A. Padlan, and D. H. Margulies. 1993. H-2Dd exploits a four residue peptide binding motif. *J. Exp. Med*. 178:1877–1892.
19. Jorgensen, J. L., U. Esser, B. Fazekas de St Groth, P. A. Reay, and M. M. Davis. 1992. Mapping T-cell receptor-peptide contacts by variant peptide immunization of single-chain transgenics. *Nature*. 355:224–230.
20. Cease, K. B., H. Margalit, J. L. Cornette, S. D. Putney, W. G. Robey, C. Ouyang, H. Z. Streicher, P. J. Fischinger, R. C. Gallo, C. DeLisi, and J. A. Berzofsky. 1987. Helper T-cell antigenic site identification in the acquired immunodeficiency syndrome virus gp120 envelope protein and induction of immunity in mice to the native protein using a 16-residue synthetic peptide. *Proc. Natl. Acad. Sci. USA*. 84:4249–4253.
21. Boehncke, W. H., T. Takeshita, C. D. Pendleton, R. A. Houghten, S. Sadegh-Nasseri, L. Racioppi, J. A. Berzofsky, and R. N. Germain. 1993. The importance of dominant negative effects of amino acid side chain substitution in peptide-MHC molecule interactions and T cell recognition. *J. Immunol*. 150:331–341.
22. Zhang, W., S. Honda, F. Wang, T. P. DiLorenzo, A. M. Kalergis, D. A. Ostrov, and S. G. Nathenson. 2001. Immunobiological analysis of TCR single-chain transgenic mice reveals new possibilities for interaction between CDR3alpha and an antigenic peptide bound to MHC class I. *J. Immunol*. 167:4396–4404.
23. Takahashi, H., Y. Nakagawa, K. Yokomuro, and J. A. Berzofsky. 1993. Induction of $CD8^+$ cytotoxic T lymphocytes by immunization with syngeneic irradiated HIV-1 envelope derived peptide-pulsed dendritic cells. *Int. Immunol*. 5:849–857.
24. Takahashi, H., Y. Nakagawa, G. R. Leggatt, Y. Ishida, T. Saito, K. Yokomuro, and J. A. Berzofsky. 1996. Inactivation of human immunodeficiency virus (HIV)-1 envelope-specific $CD8^+$ cytotoxic T lymphocytes by free antigenic peptide: a self-veto mechanism? *J. Exp. Med*. 183:879–889.
25. Margulies, D. H., G. A. Evans, K. Ozato, R. D. Camerini-Otero, K. Tanaka, E. Appella, and J. G. Seidman. 1983. Expression of H-2Dd and H-2Ld mouse major histocompatibility antigen genes in L cells after DNA-mediated gene transfer. *J. Immunol*. 130:463–470.
26. Abastado, J.P., C. Jaulin, M.P. Schutze, P. Langlade_Demoyen, F. Plata, K. Ozato, and P. Kourilsky. 1987. Fine mapping of epitopes by intradomain K^d/D^d recombinants. *J. Exp. Med*. 166:327–340.
27. Takahashi, M., E. Osono, Y. Nakagawa, J. Wang, J. A. Berzofsky, D. H. Margulies, and H. Takahashi. 2002. Rapid induction of apoptosis in $CD8^+$ HIV-1 envelope-specific murine CTLs by short exposure to antigenic peptide. *J. Immunol*. 169:6588–6593.